ISSN 0280–5316
ISRN LUTFD2/TFRT--5535--SE

Singularly Perturbed Systems

Hélène Panagopoulos

Department of Automatic Control
Lund Institute of Technology
August 1995

Department of Automatic Control
Lund Institute of Technology
P.O. Box 118
S-221 00 Lund Sweden

Document name
MASTER THESIS

Date of issue
August 1995

Document Number
ISRN LUTFD2/TFRT--5535--SE

Author(s)
Hélène Panagopoulos

Supervisor
Rolf Johansson, Anders Robertsson

Sponsoring organisation

Title and subtitle

Singularly Perturbed Systems

Abstract

Usually, when we analyze a complex dynamical system we prefer to work with a reduced-order model, by neglecting small parasitic parameters which increase the order of the model. This model simplification may not always be legitimate. For instance, if the dynamics associated with the parasitic elements were unstable, we should not have neglected them in the first place.

The theory of singular perturbations provides a stability theorem to find out for which values of ϵ it will be justified to only work with the simplified model. The main theme of this master thesis is to investigate this theorem in the sense of examining how applicable it is to an arbitrary problem and to see if it is possible to generalize it. Hopefully, our results may contribute with some valuable insights for other scientists.

Key words

Classification system and/or index terms (if any)

Supplementary bibliographical information

ISSN and key title
0280–5316

ISBN

Language
English

Number of pages
52

Recipient's notes

Security classification

Abstract

Usually, when we analyze a complex dynamical system we prefer to work with a reduced-order model, by neglecting small parasitic parameters which increase the order of the model. This model simplification may not always be legitimate. For instance, if the dynamics associated with the parasitic elements were unstable, we should not have neglected them in the first place.
The theory of singular perturbations provides a stability theorem to find out for which values of ϵ it will be justified to only work with the simplified model. The main theme of this master thesis is to investigate this theorem in the sense of examining how applicable it is to an arbitrary problem and to see if it is possible to generalize it. Hopefully, our results may contribute with some valuable insights for other scientists.

Contents

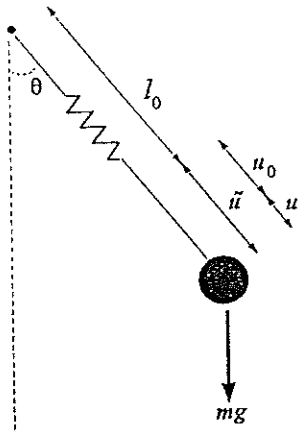

Figure 0.1: The Pendulum

Introduction

Quite often in the analysis of dynamical systems we use reduced-order models obtained by neglecting small time constants, masses, capacitances and similar "parasitic" parameters which increase the order of the model. The theory of singular perturbations legitimizes this model simplification and provides tools for improving oversimplified models. By setting up a singularly perturbed model representing the actual system with the parasitic parameters, denoted ϵ, we will get a convenient way of decomposing the model into a reduced (slow) model and a boundary-layer (fast) model.
Modelling a physical system into a singularly perturbed form may be difficult. It is not always clear how to choose parameters that will be considered as small. Fortunately, in many applications our knowledge of physical processes and components of the system sets us on the right track. To get a profound understanding of how to set up a singularly perturbed model, we will first give a short review of the theory of singular perturbations. Thereafter, a singularly perturbed model of the energy conservative pendulum, Figure 0.1, will be set up. Consequently, we can show how easy it is to have it decomposed into a reduced model and a boundary-layer model. For this case we take $\frac{1}{\sqrt{k}}$ as the "parasitic" parameter ϵ, where k is the spring constant.

The theory of singular perturbations provides means in finding those ϵ for which the singular pertubation model is asymptotically stable. This implies that it will be legitimate in the analysis of the dynamical system just to work with the reduced system for these ϵ. Theorem B.1, in appendix B, tells us how to find these ϵ for our singularly perturbed model. Consequently, the conditions of the theorem will be our guide-lines to find those ϵ for which the singularly perturbed model of the pendulum is asymptotically stable. For the energy conservative pendulum the conditions of the theorem will not be fulfilled. On the

contrary, the introduction of resisting forces in the dynamics of the pendulum will generate a singularly perturbed model, which will fulfill the conditions of Theorem B.1, thus, giving us an upper bound for ϵ. By means of the simulation tool Omsim we can verify if the energy dissipative pendulum will have an asymptotically stable behaviour for those ϵ given by Theorem B.1.
An interesting question arises on the possibility of generalizing Theorem B.1, in the sence of neglecting some of the conditions in the proof of the theorem. As a result, the upper bound of ϵ will be raised, implying a broadening of the interval of possible ϵ which may generate an asymptotically stable behaviour of the singularly perturbed system. We will try to answer this question by examining a set of dynamical systems, where one of them is the previously mentioned energy dissipative pendulum.

Chapter 1

The Theory of Autonomous Singularly Perturbed Systems

To obtain a comprehensive result of this report, a short introduction of the theory of autonomous singularly perturbed systems is given. A more thorough analysis of the theory may be found in [4], Chapter 8.
The singular perturbation model of a dynamical system is a state-space model in which the derivatives of some of the states are multiplied by a small positive parameter ϵ, that is,

$$\dot{x} = f(x, z, \epsilon), \qquad x \in R^n, \tag{1.1}$$

$$\epsilon \dot{z} = g(x, z, \epsilon), \qquad z \in R^m. \tag{1.2}$$

We assume that the functions f and g are continuously differentiable in their arguments for $(x, z, \epsilon) \in D_1 \times D_2 \times [0, \epsilon_0]$, where $D_1 \subset R^n$ and $D_2 \subset R^m$ are open connected sets. When we set $\epsilon = 0$ in (1.1)-(1.2), the dimension of the state equation reduces from $n + m$ to n because the differential equation (1.2) degenerates into the equation

$$0 = g(x, z, 0). \tag{1.3}$$

The model (1.1)-(1.2) is in standard form if and only if the equation (1.3) has $p \geq 1$ isolated roots

$$z = h_i(x), \qquad i = 1, 2, \ldots, p \tag{1.4}$$

for each $x \in D_1$. This assumption ensures that a well-defined n-dimensional reduced model will correspond to each root of (1.3). To obtain the ith reduced

model, we substitute (1.4) into (1.1), at $\epsilon = 0$, to obtain

$$\dot{x} = f(x, h(x), 0) \tag{1.5}$$

where we have dropped the subscript i from h. (1.5) is also known as the *slow model.*
It is more convenient in the analysis to perform the change of variables

$$y = z - h(x)$$

that shifts the quasi-steady-state of z to the origin. In the new variables (x, y), the full problem is

$$\dot{x} = f(x, y + h(x), \epsilon), \tag{1.6}$$

$$\epsilon\dot{y} = g(x, y + h(x), \epsilon) - \epsilon\frac{\partial h}{\partial x} f(x, y + h(x), \epsilon). \tag{1.7}$$

The quasi-steady-state of (1.7) is now $y = 0$, which when substituted in (1.6) results in the reduced model (1.5).
To analyse (1.7), let us note that $\epsilon\dot{y}$ may remain finite even when ϵ tends to zero and $\dot{y}$ tends to infinity. We set $\epsilon\frac{dy}{dt} = \frac{dy}{d\tau}$, hence $\frac{d\tau}{dt} = \frac{1}{\epsilon}$ and use $\tau = 0$ as the initial value at $t = t_0$, where t_0 is the initial value of the system equations (1.6) and (1.7). The new time variable $\tau = (t - t_0)/\epsilon$ is "stretched"; that is, if ϵ tends to zero, τ tends to infinity even for finite differences $t - t_0$ (which is independant of ϵ). In the τ time scale, equation (1.7) is represented by

$$\frac{dy}{d\tau} = g(x, y + h(x), \epsilon) - \epsilon\frac{\partial h}{\partial x} f(x, y + h(x), \epsilon). \tag{1.8}$$

Consequently, the variables t and x in the foregoing equation will be slowly varying since, in the τ time scale, they are given by

$$t = t_0 + \epsilon\tau,$$
$$x = x(t_0 + \epsilon\tau, \epsilon).$$

Setting $\epsilon = 0$ freezes these variables, that is they can be considered to be constant in the fast time scale, and reduces (1.8) to

$$\frac{dy}{d\tau} = g(x, y + h(x), 0) \tag{1.9}$$

which we refer to as *the boundary-layer system*, also known as the fast system.

Chapter 2

The Singularly Perturbed System of the Energy Conservative Pendulum

After the short introduction on the theory of singular perturbations we will now set up a singularly perturbed model of the pendulum in Figure 0.1. Thereafter, we wish to find out wheather Theorem B.1 can be applied to it or not.
Consider the pendulum, shown in Figure 0.1, where l_0 denotes the length of the rod without a bob applied to it. Here m denotes the mass of the bob. Assume the rod has zero mass. Let θ denote the angle subtended by the rod and the vertical axis through the pivot point, we assume $-\pi < \theta < \pi$. The pendulum is free to swing in the vertical plane, thus the bob moves in a circle of radius $l_0+\tilde{u}$, where $\tilde{u} = u+u_0$. u_0 is the extension of the spring at equilibrium ($\theta = 0, u = 0$). u is the extension of the spring aside the equilibrium length when the pendulum is in motion. To write the equation of motion of the pendulum, let us consider the displacement of the bob along the rod and the motion of the bob in the tangential direction. We assume the system is conservative in the sense that if the pendulum is given an initial push, it will keep oscillating forever, with a nondissipative energy exchange between kinetic and potential energies.

2.1 The Model Equation of the Bob in the Mass-Spring System

To write the equation of the motion of the bob in the mass-spring system, let us identify the forces acting on the bob, see Figure 2.1. There is a restoring force of the spring, F_{sp}, equal to $k\tilde{u}$ where k is the spring constant. There is also the downward gravitational force F equal to $mg\cos\theta$, where g is the acceleration

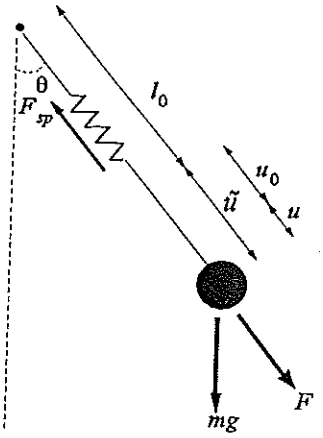

Figure 2.1: Mass-spring mechanical system

due to gravity. Using Newton's second law of motion, we can write the equation of the mass-spring mechanical system as

$$m\ddot{\tilde{u}} + F_{sp} = F$$

that is

$$\frac{1}{k}\ddot{\tilde{u}} = \frac{g}{k}\cos\theta - \frac{1}{m}\tilde{u}. \tag{2.1}$$

2.1.1 The Displacement of the Bob at Equilibrium

We rewrite (2.1) in a state space equation to find the displacement of the bob at equilibrium, that is u_0. Set $\xi_1 = \tilde{u}$ and $\xi_2 = \dot{\tilde{u}}$ then (2.1) becomes

$$\begin{cases} \dot{\xi}_1 = \xi_2, \\ \dot{\xi}_2 = g\cos\theta - \frac{k}{m}\xi_1. \end{cases}$$

Thus, the equilibrium is $(\xi_1, \xi_2) = (\frac{mg}{k}, 0)$. As $\tilde{u} = u + u_0$ we can rewrite equation (2.1) as

$$\frac{1}{k}\ddot{u} = \frac{g}{k}(\cos\theta - 1) - \frac{1}{m}u.$$

2.2 The Model Equation of the Bob in the Tangential Direction

To write the equation of the motion of the bob in the tangential direction, let us identify the forces acting on the bob, see Figure 2.2. According to the

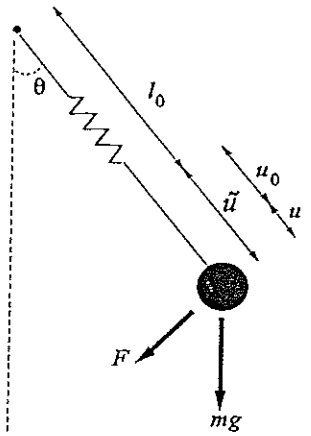

Figure 2.2: The motion of the bob in the tangential direction

assumption we have an energy conservative system, that is, no frictional forces acts on the the tangential motion of the bob. Therefore, the only force acting on the bob is the downward gravitational force F equal to $mg\sin\theta$, where g is the acceleration due to gravity. We calculate the motion of the bob in the tangential direction from the torque τ through the suspension point,

$$\tau = -rF \tag{2.2}$$

where r, the lever arm, is equal to $(l_0 + u_0 + u)$. The torque is given by

$$\tau = I\alpha_T \tag{2.3}$$

where I is the moment of inertia and α_T is the angular acceleration. That is

$$I = m(l_0 + u_0 + u)^2, \tag{2.4}$$

$$\alpha_T = \frac{1}{(l_0 + u_0 + u)}(\dot{u}\,\dot{\theta} + (l_0 + u_0 + u)\,\ddot{\theta}). \tag{2.5}$$

From equation (2.2) - (2.5) we get the model equation of the tangential motion of the bob. That is,

$$I\alpha_T = -rF,$$

thus

$$\ddot{\theta} = -\frac{g}{(l_0 + u_0 + u)}\sin\theta - \frac{1}{(l_0 + u_0 + u)}\dot{u}\,\dot{\theta}.$$

2.3 The Singularly Perturbed Model of the Energy Conservative Pendulum

From the results in Section 2.1 and 2.2 we can now write the dynamical equations of the energy conservative pendulum, that is

$$\begin{cases} \ddot{\theta} &= -\frac{1}{(l_0+u_0+u)}g\sin\theta - \frac{1}{(l_0+u_0+u)}\dot{u}\dot{\theta}, \\ \frac{1}{k}\ddot{u} &= \frac{g}{k}(\cos\theta - 1) - \frac{1}{m}u. \end{cases}$$

We have arrived to the crucial point where the parasitic parameter ϵ shall be chosen so that the dynamical equations of the pendulum can be written in singularly perturbed form. We choose ϵ to $\frac{1}{\sqrt{k}}$, where k is the spring constant. For large k:s the spring gets stiffer and stiffer, which is the same as considering the total system of the rod and spring as one single stiff rod, that is, neglecting the dynamics of the spring.
Introduce the state variables and the parameter $\epsilon = \frac{1}{\sqrt{k}}$

$$\begin{cases} x_1 = \theta, \\ x_2 = \dot{\theta}, \\ z_1 = u, \\ z_2 = \epsilon\dot{u}. \end{cases}$$

Then, the state equation is given by

$$\begin{aligned} \dot{x}_1 &= x_2, \\ \dot{x}_2 &= -\frac{g}{(l_0 + \epsilon^2 mg + z_1)}\sin x_1 - \frac{1}{(l_0 + \epsilon^2 mg + z_1)\epsilon}z_2 x_2, \\ \epsilon\dot{z}_1 &= z_2, \\ \epsilon\dot{z}_2 &= \epsilon^2 g(\cos x_1 - 1) - \frac{1}{m}z_1 \end{aligned} \tag{2.6}$$

which is represented in standard singular perturbed form, that is,

$$\begin{aligned} \dot{x} &= f(x, z, \epsilon), \qquad x \in R^2, \\ \epsilon\dot{z} &= g(x, z, \epsilon), \qquad z \in R^2. \end{aligned}$$

The equilibrium point of the singularly perturbed system is $(x_1^0, x_2^0, z_1^0, z_2^0) = (0, 0, 0, 0)$.
Setting $\epsilon = 0$ in (2.6) yields the equation system

$$\begin{cases} 0 = z_2, \\ 0 = -\frac{1}{m}z_1, \end{cases}$$

which has an unique root $z = h(x) = \begin{bmatrix} 0 & 0 \end{bmatrix}^T$.

To be consistent with the notations in Chapter 1, we make the variable shift $y = z$. Thus the reduced model, $\dot{x} = f(x, h(x))$, is

$$\begin{cases} \dot{x}_1 = x_2, \\ \dot{x}_2 = -\frac{g}{l_0} \sin x_1, \end{cases}$$

with the equilibrium point $(x_1^0, x_2^0) = (0, 0)$, and the boundary-layer model, $\frac{dy}{d\tau} = g(x, y + h(x))$, is

$$\begin{cases} \frac{dy_1}{d\tau} = y_2, \\ \frac{dy_2}{d\tau} = -\frac{1}{m} y_1, \end{cases}$$

with the equilibrium point $(y_1^0, y_2^0) = (0, 0)$.

2.4 Stability of the Energy Conservative Pendulum

We will now try to find the ϵ applicable to the energy conservative pendulum for which the singularly perturbed model (2.6) is asymptotically stable. We will succeed if we can fulfill the conditions of Theorem B.1 in appendix B. Let us start by studying the origins of the reduced and the boundary-layer system, searching for Lyapunov functions $V(x)$ and $W(x, y)$ which satisfies (B.7)-(B.9).

2.4.1 Stability of the Reduced System

Consider the slow system

$$\begin{cases} \dot{x}_1 = x_2, \\ \dot{x}_2 = -\frac{g}{l_0} \sin x_1. \end{cases}$$

Let us study the stability of the equilibrium point at the origin. A natural Lyapunov candidate is the energy function

$$V(x) = \frac{g}{l_0}(1 - \cos x_1) + \frac{1}{2} x_2^2,$$

according to [4], p.106. Clearly, $V(0) = 0$ and $V(x)$ are positive definite over the domain $-\pi < x_1 < \pi$. The derivative of $V(x)$ along the trajectoires of the system is given by

$$\dot{V}(x) = \frac{g}{l_0} \dot{x}_1 \sin x_1 + x_2 \dot{x}_2 = \frac{g}{l_0} x_2 \sin x_1 - \frac{g}{l_0} x_2 \sin x_1 = 0.$$

Thus $V(x)$ satisfies (A.1) and (A.2) of Theorem A.1, see appendix A, and we can conclude that the origin is stable but not asymptotically stable which was the request of Theorem B.1.

2.4.2 Stability of the Boundary-Layer System

Consider the fast system

$$\begin{cases} \dot{y}_1 = y_2, \\ \dot{y}_2 = -\frac{1}{m} y_1. \end{cases}$$

This is a linear system whith the system matrix A

$$A = \begin{bmatrix} 0 & 1 \\ -\frac{1}{m} & 0 \end{bmatrix}$$

which has the eigenvalues $\lambda_{1,2} = \pm i\sqrt{\frac{1}{m}}$. As the $Re\,\lambda_j = 0$, $j = 1, 2$, Theorem A.2, see appendix A, will imply that the linear system is stable but not asymptotically stable. According to Theorem A.3, see appendix A, we can not find a Lyapunov function which fulfills the requests of Theorem B.1.
As the boundary-layer model is a linear system we can calculate its solution

$$y(\tau) = y(0) S e^{\Lambda \tau} S^{-1}$$

where $A = S^{-1}\Lambda S$. After some calculations we can write the solution as

$$y_1(\tau) = y_1(0)\cos\tau\sqrt{\frac{1}{m}} - y_2(0)\sqrt{m}\sin\tau\sqrt{\frac{1}{m}}, \tag{2.7}$$

$$y_2(\tau) = y_1(0)\frac{1}{\sqrt{m}}\sin\tau\sqrt{\frac{1}{m}} + y_2(0)\sqrt{m}\cos\tau\sqrt{\frac{1}{m}}. \tag{2.8}$$

From (2.7)-(2.8) we see that the boundary-layer system is a stable oscillating system but not asymptotically stable, which confirms the conclusions of Theorem A.3.

Conclusion of the Stability of the Energy Conservative Pendulum

We can not apply Theorem B.1 to our dynamical system, because the reduced and the boundary-layer model are not asymptotically stable in their origin. Consequently, we can not find any ϵ for which the origin of the singularly perturbed model of the energy conservative pendulum is asymptotically stable.
According to our simulations in OmSim the dynamical system of the energy conservative pendulum for different spring constants k, is not asymptotically stable, but it is stable, see Figure 2.3 and Figure 2.4.

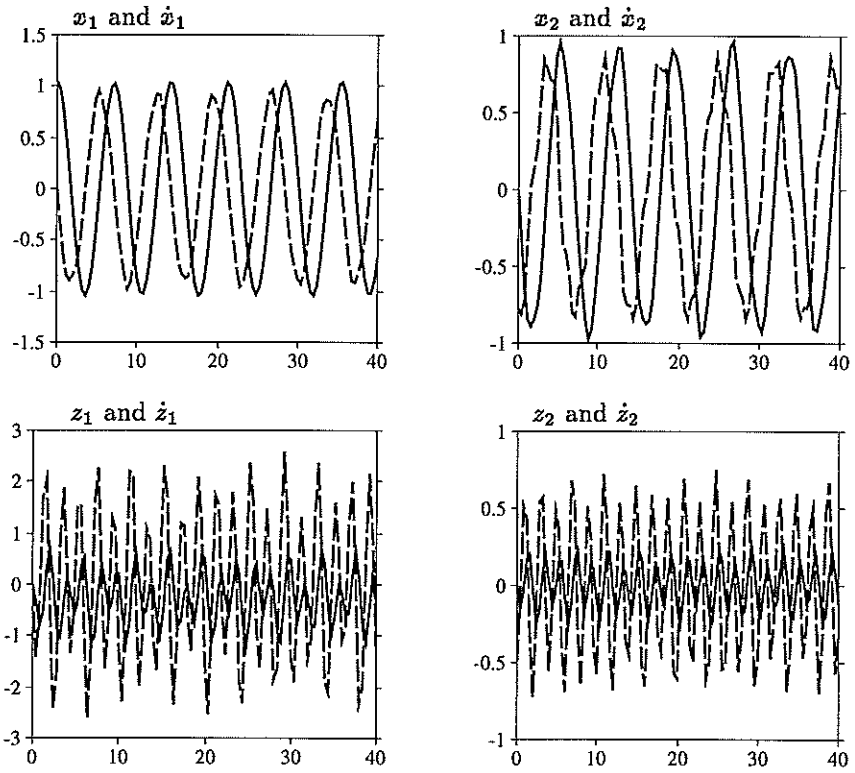

Figure 2.3: Simulation of the energy conservative pendulum for $\epsilon = 0.1$, $l_0 = 10$, $m = 10, x_1(0) = 1.047$, $\dot{x}_1(0) = 0$, $x_2(0) = 0$, $\dot{x}_2(0) = 0$, $z_1(0) = 0$, $\dot{z}_1(0) = 0$, $z_2(0) = 0$, $\dot{z}_2(0) = 0$. The solid lines show x_1, x_2, z_1 and z_2, while the dashed lines show their respective derivatives

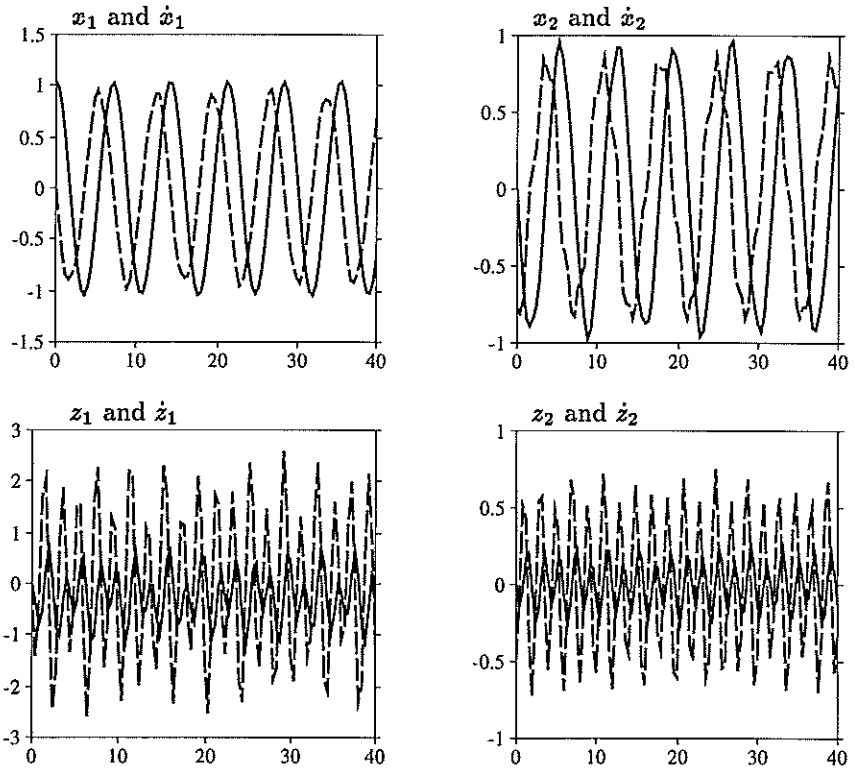

Figure 2.4: Simulation of the energy conservative pendulum for $\epsilon = 1$, $l_0 = 10$, $m = 10, x_1(0) = 1.047$, $\dot{x}_1(0) = 0$, $x_2(0) = 0$, $\dot{x}_2(0) = 0$, $z_1(0) = 0$, $\dot{z}_1(0) = 0$, $z_2(0) = 0$, $\dot{z}_2(0) = 0$. The solid lines show x_1, x_2, z_1 and z_2, while the dashed lines show their respective derivatives.

Chapter 3

The Singularly Perturbed Model of the Energy Dissipative Pendulum

In the previous chapter we saw that there is no possibility to fulfill the demands of Theorem B for the energy conservative pendulum, that is, finding a reduced model and a boundary-layer model which are asymptotically stable in their equilibrium point. This chapter will show how the introduction of resisting forces in the dynamic of the pendulum will produce a reduced and a boundary-layer model which are asymptotically stable in their equilibrium points. As a result, we can use Theorem B.1 to calculate the upper bound of ϵ for which the singularly perturbed model of the energy dissipative pendulum is asymptotically stable at the origin. By means of the simulation tool OmSim we will verify if our theoretical results will agree with the simulated ones.

3.1 The Model Equation of the Mass-Spring System

To write the equation of the motion of the bob in the tangential direction we will proceede as in Section 2.1. Let us identify the forces acting on the bob, see Figure 3.1. To begin with, there is the restoring force of the spring, F_{sp}, equal to $k\tilde{u}$ where k is the spring constant and $\tilde{u} = u + u_0$. In this case we also have a frictional force due to viscosity. This force is usually modelled as a nonlinear function of the velocity, that is $F_v = v(\dot{\tilde{u}})$, where $v(0) = 0$. We assume small velocities, why $F_v = \alpha\sqrt{k}\dot{\tilde{u}}$, where $\alpha < 1$ is a small positive parameter. Finally there is the downward gravitational force F equal to $mg\cos\theta$, where g denotes the acceleration due to gravity. Using Newton's second law of motion, we can

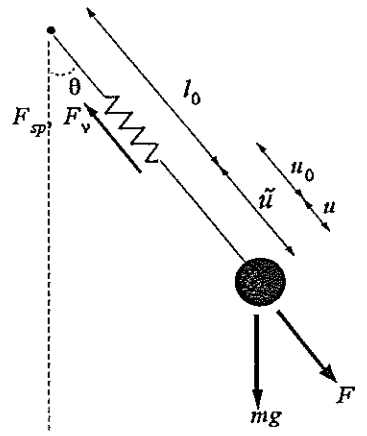

Figure 3.1: The mass-spring mechanical system.

write the equation of the mass-spring mechanical system as

$$m\ddot{\tilde{u}} + F_{sp} + F_{\nu} = F$$

that is

$$\frac{1}{k}\ddot{\tilde{u}} = \frac{g}{k}\cos\theta - \frac{1}{m}\tilde{u} - \frac{\alpha}{\sqrt{k}}\dot{\tilde{u}}. \tag{3.1}$$

3.1.1 The Displacement of the Bob at Equilibrium

In the same way as in Subsection 2.1.1 we can rewrite (3.1) in a state space equation to find the displacement of the bob at equilibrium, that is u_0. Set $\xi_1 = \tilde{u}$ and $\xi_2 = \dot{\tilde{u}}$ then (3.1) becomes

$$\begin{cases} \dot{\xi}_1 = \xi_2, \\ \dot{\xi}_2 = g\cos\theta - \frac{k}{m}\xi_1 - \frac{\alpha}{\sqrt{k}}\xi_2. \end{cases}$$

Thus, the equilibrium is $(\xi_1, \xi_2) = (\frac{mg}{k}, 0)$.
As $\tilde{u} = u + u_0$ we can rewrite equation (3.1),

$$\frac{1}{k}\ddot{u} = \frac{g}{k}(\cos\theta - 1) - \frac{1}{m}u - \frac{\alpha}{\sqrt{k}}\dot{u}.$$

3.2 The Model Equation of the Bob's Motion in the Tangential Direction

To write the equation of the motion of the bob in the tangential direction we proceed in the same way as we did in Section 2.2 except for the introduced

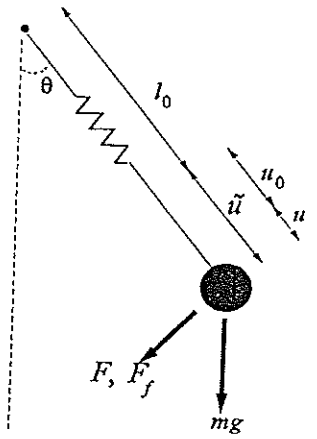

Figure 3.2: The motion of the bob in the tangential direction.

frictional force. Let us identify the forces acting on the bob, see Figure 3.2. To begin with there is the frictional force F_f equal to ηv_T, where η is a frictional coefficient and v_T is the tangential velocity. That is

$$F_f = \eta v_T = \eta(l_0 + u_0 + u)\dot{\theta}. \tag{3.2}$$

Finally we have the downward gravitational force, F, equal to $mg\sin\theta$, where g denotes the acceleration due to gravity.
We calculate the motion of the bob in the tangential direction from the torque τ through the suspension point,

$$\tau = r\,(-F - F_f), \tag{3.3}$$

where r, the lever arm, is equal to $(l_0 + u_0 + u)$. The torque is given by

$$\tau = I\alpha_T \tag{3.4}$$

where I is the moment of inertia and α_T is the angular acceleration. That is

$$I = m\,(l_0 + u_0 + u)^2, \tag{3.5}$$

$$\alpha_T = \frac{1}{(l_0 + u_0 + u)}(\dot{u}\,\dot{\theta} + (l_0 + u_0 + u)\,\ddot{\theta}). \tag{3.6}$$

From equations (3.2)-(3.3) we get the model equation of the tangential motion of the bob. That is,

$$I\alpha_T = r\,(-F - F_f)$$

thus

$$\ddot{\theta} = -\frac{g}{(l_0 + u_0 + u)}\sin\theta - \frac{1}{(l_0 + u_0 + u)}\dot{u}\,\dot{\theta} - \frac{\eta}{m}\dot{\theta}.$$

3.3 The Singularly Perturbed Model of the Pendulum

According to the results in Section 3.1 and 3.2 we can now write the dynamical equations of the energy conservative pendulum, that is

$$\begin{cases} \ddot{\theta} &= -\frac{1}{(l_0+u_0+u)} g \sin\theta - \frac{1}{(l_0+u_0+u)} \dot{u}\dot{\theta} - \frac{\eta}{m}\dot{\theta}, \\ \frac{1}{k}\ddot{u} &= \frac{g}{k}(\cos\theta - 1) - \frac{1}{m}u - \frac{\alpha}{\sqrt{k}}\dot{u}. \end{cases}$$

The dynamical equations of the pendulum can now be rewritten into singularly perturbed form by choosing ϵ and the state variables as in Section 2.3, that is,

$$\begin{cases} x_1 = \theta, \\ x_2 = \dot{\theta}, \\ z_1 = u, \\ z_2 = \epsilon\dot{u} \end{cases}$$

where $\epsilon = \frac{1}{\sqrt{k}}$. Then, the state equation is given by

$$\begin{aligned} \dot{x}_1 &= x_2, \\ \dot{x}_2 &= -\frac{g}{(l_0 + \epsilon^2 mg + z_1)} \sin x_1 - \frac{1}{(l_0 + \epsilon^2 mg + z_1)} \frac{z_2}{\epsilon} x_2 - \frac{\eta}{m} x_2, \\ \epsilon\dot{z}_1 &= z_2, \\ \epsilon\dot{z}_2 &= \epsilon^2 g(\cos x_1 - 1) - \frac{1}{m} z_1 - \alpha z_2. \end{aligned} \tag{3.7}$$

which is represented in standard singularly perturbed form, that is,

$$\begin{aligned} \dot{x} &= f(x, z, \epsilon), \qquad x \in R^2 \\ \epsilon\dot{z} &= g(x, z, \epsilon), \qquad z \in R^2 \end{aligned}$$

The equilibrium point of the singularly perturbed system is $(x_1^0, x_2^0, z_1^0, z_2^0) = (0, 0, 0, 0)$.
Setting $\epsilon = 0$ in (3.7) yields the equation system

$$\begin{cases} 0 = z_2, \\ 0 = -\frac{1}{m} z_1 - \alpha z_2, \end{cases}$$

which has an unique root $z = h(x) = \begin{bmatrix} 0 & 0 \end{bmatrix}^T$. To be consistent with the notations in Chapter 1 we make the variable shift $y = z$. Thus the reduced model, $\dot{x} = f(x, h(x))$, is

$$\begin{cases} \dot{x}_1 = x_2, \\ \dot{x}_2 = -\frac{g}{l_0} \sin x_1 - \frac{\eta}{m} x_2. \end{cases}$$

with the equilibrium point $(x_1^0, x_2^0) = (0, 0)$ and the boundary-layer model, $\frac{dy}{d\tau} = g(x, y + h(x))$, is

$$\begin{cases} \frac{dy_1}{d\tau} = y_2, \\ \frac{dy_2}{d\tau} = -\frac{1}{m}y_1 - \alpha y_2. \end{cases}$$

with the equilibrium point $(y_1^0, y_2^0) = (0, 0)$.

3.4 Stability of the Energy Dissipative Pendulum

Now we have arrived to the purpose of this chapter, which is to find those ϵ for which the singularly perturbed model (3.7) is asymptotically stable at the origin. Consequently, we want to satisfy the conditions in Theorem B. Until now we have constructed our model so that it will be possible to find Lyapunov functions $V(x)$ and $W(x, y)$ for the reduced model and the boundary-layer model respectively. Firstly we will derive these Lyapunov functions as they are fundamental in the further analysis to fulfill the conditions in the theorem.
Secondly, we will examine if our found Lyapunov functions will satisfy the conditions of (B.7)-(B.9) and (B.10)-(B.11)in Theorem B.1. If you recall from appendix B the conditions (B.10)-(B.11), which are referred to as the interconnection conditions, will be fulfilled if the conditions (B.15)-(B.19) are valid, that is

$$\begin{aligned} \| \frac{\partial V}{\partial x} \| &\leq k_1\psi_1(x), \\ \| f(x, h(x)) \| &\leq k_2\psi_1(x), \\ \| f(x, y + h(x)) - f(x, h(x)) \| &\leq k_3\psi_2(y), \\ \| \frac{\partial W}{\partial y} \| &\leq k_4\psi_2(y), \\ \| \frac{\partial W}{\partial x} \| &\leq k_5\psi_2(y). \end{aligned}$$

Finally, if all these conditions are fulfilled, we can conclude that the origin is asymptotically stable for $\epsilon < \epsilon^*$. If so, we wish to verify if the upper bound ϵ^* will be legitimate by simulating the dynamical system of the pendulum for different $\epsilon < \epsilon^*$, in OmSim.

3.4.1 Stability of the Reduced System

Consider the slow system

$$\begin{cases} \dot{x}_1 = x_2, \\ \dot{x}_2 = -\frac{g}{l_0}\sin x_1 - \frac{\eta}{m}x_2. \end{cases}$$

Let us study the stability of the equilibrium point at the origin. According to reasoning in [4] p.106-107 the following Lyapunov candidate,

$$V(x) = \frac{1}{2}x^T \begin{bmatrix} \frac{1}{2}a^2 & \frac{1}{2}a \\ \frac{1}{2}a & 1 \end{bmatrix} x + \left(\frac{g}{l_0}\right)(1 - \cos x_1),$$

where $a = \left(\frac{\eta}{m}\right)$, will in the domain $D = \{x \in R^2;\ |x_1| < \pi\}$, satisfies the conditions (A.1)-(A.2), in Theorem A.1. Thus, the origin of the reduced system is asymptotically stable.

3.4.2 Stability of the Boundary-Layer System

Consider the fast system

$$\begin{cases} \dot{y}_1 = y_2, \\ \dot{y}_2 = -\frac{1}{m}y_1 - \alpha y_2. \end{cases}$$

Routh's algorithm gives us that for $\alpha > 0$ the boundary-layer system is asymptotically stable. Consequently the system marix is a stability matrix.
Let P be the solution of the Lyapunov equation

$$PA + A^T P = -I,$$

where A is the system matrix, P is a symmetric, positive definite matrix and I is the identity matrix. It is given by

$$P = \begin{bmatrix} p_{11} & p_{12} \\ p_{12} & p_{22} \end{bmatrix}$$

where

$$\begin{cases} p_{11} = \frac{m}{2}\left(\alpha + \frac{m+1}{\alpha m^2}\right), \\ p_{12} = \frac{m}{2}, \\ p_{22} = \frac{m+1}{2\alpha}. \end{cases}$$

Consequently, the Lyapunov function to the boundary-layer system is $W(x, y) = y^T P y$, that is

$$W(x, y) = y^T \begin{bmatrix} \frac{m}{2}\left(\alpha + \frac{m+1}{\alpha m^2}\right) & \frac{m}{2} \\ \frac{m}{2} & \frac{m+1}{2\alpha} \end{bmatrix} y.$$

3.4.3 Finding the Upper Bound of ϵ

In the previous two subsections we have found two Lyapunov functions $V(x)$ and $W(x, y)$, we will now check if they satisfy the conditions (B.7)-(B.9) in Theorem B.1 and (B.15)-(B.19) in appendix B. The last one is a smoother way to fulfill the interconnection conditions of the theorem. Notice that we do not

need to estimate the conditions (B.16), (B.18) and (B.19), because our functions $W(x,y)$ and $h(x)$ do not depend on x. Consequently, the interconnection condition (B.11) is equal to zero, that is

$$\left[\frac{\partial W}{\partial x} - \frac{\partial W}{\partial y}\frac{\partial h}{\partial x}\right] f(x,h(x)) = 0.$$

3.4.4 The Upper Bound of $\frac{\partial V}{\partial x} f(x,h(x))$

The reduced system $f(x,h(x))$, is

$$f(x,h(x)) = \begin{bmatrix} x_2 \\ -\left(\frac{g}{l_0}\right)\sin x_1 - \left(\frac{\eta}{m}\right) x_2 \end{bmatrix}$$

where g, η, l_0 and $m > 0$. The Lyapunov function of the reduced system is

$$V(x) = \frac{1}{4}\left(\frac{\eta}{m}\right)^2 x_1^2 + \frac{1}{2}\left(\frac{\eta}{m}\right) x_1 x_2 + \frac{1}{2}x_2^2 + \left(\frac{g}{l_0}\right)(1-\cos x_1).$$

The partial derivative of $V(x)$ is,

$$\frac{\partial V}{\partial x} = \begin{bmatrix} \frac{1}{2}\left(\frac{\eta}{m}\right)^2 x_1 + \frac{1}{2}\left(\frac{\eta}{m}\right) x_2 + \left(\frac{g}{l_0}\right)\sin x_1 & \frac{1}{2}\left(\frac{\eta}{m}\right) x_1 + x_2 \end{bmatrix}.$$

We wish to find the upper bound of $\frac{\partial V}{\partial x} f(x,h(x))$, that is

$$\frac{\partial V}{\partial x} f(x,h(x)) = -\frac{1}{2}\left(\frac{\eta}{m}\right)\left(\frac{g}{l_0}\right) x_1 \sin x_1 - \frac{1}{2}\left(\frac{\eta}{m}\right) x_2^2.$$

Set $a = \frac{\eta}{m}$, $b = \frac{g}{l_0}$.
First examine the lower bound of $b|x_1|\sin|x_1| + |x_2|^2$, where $|x_1| < \pi$, $|x_2| > 0$. Introduce the restriction $|x_1| < \pi - \delta$, where δ is a small positive constant. We know from [5] that

$$\frac{2}{\pi} \leq \frac{\sin x_1}{x_1} \leq 1, 0 < x_1 \leq \frac{\pi}{2}. \tag{3.8}$$

The inequality relation is symmetric with respect to x_1 why (3.8) is also valid for $-\frac{\pi}{2} \leq x_1 < 0$. For $\frac{\pi}{2} < x_1 \leq \pi - \delta_1$ we make the variable translation $x_1 = \pi - x_1$. Then we can rewrite (3.8) as

$$\frac{2}{\pi} \leq \frac{\sin x_1}{\pi - x_1} \leq 1, \frac{\pi}{2} < x_1 \leq \pi. \tag{3.9}$$

The inequality relation is symmetric with respect to x_1 why (3.9) is also valid for $-\pi < x_1 \leq -\frac{\pi}{2}$. We begin by searching for the lower bound of $b|x_1|\sin|x_1| +$

$|x_2|^2$, for the case $0 < |x_1| \leq \frac{\pi}{2},\ |x_2| > 0$.

$$\begin{aligned} & b|x_1|\sin|x_1| + |x_2|^2 \\ & \geq \frac{2b}{\pi}|x_1|^2 + |x_2|^2 \\ & \geq \frac{b}{\pi}\left(|x_1| + |x_2|\right)^2. \end{aligned}$$

Here b has been chosen such that $2b \leq \pi$.
Now we wish to find the lower bound of $b|x_1|\sin|x_1| + |x_2|^2$, for the case $\frac{\pi}{2} < |x_1| < \pi - \delta_1,\ |x_2| > 0$.

$$\begin{aligned} & b|x_1|\sin|x_1| + |x_2|^2 \\ & \geq \frac{2b}{\pi}(\pi - |x_1|)|x_1| + |x_2|^2 \\ & = 2b|x_1| - \frac{2b}{\pi}|x_1|^2 + |x_2|^2 \\ & \geq \left(\frac{2b}{(\pi - \delta_1)} - \frac{2b}{\pi}\right)|x_1|^2 + |x_2|^2 \\ & \geq \frac{2b\delta_1}{\pi(\pi - \delta_1)}\left(|x_1|^2 + |x_2|^2\right) \\ & \geq \frac{b\delta_1}{\pi(\pi - \delta_1)}\left(|x_1| + |x_2|\right)^2. \end{aligned}$$

Here b has been chosen such that $2b\delta_1 \leq \pi(\pi - \delta_1)$.
Thus the upper bound of $\frac{\partial V}{\partial x}f(x, h(x))$ for $|x_1| < \pi - \delta_1,\ |x_2| > 0$ is

$$\frac{\partial V}{\partial x}f(x, h(x)) \leq -\frac{\eta g \delta_1}{2ml_0\pi(\pi - \delta_1)}\left(|x_1| + |x_2|\right)^2.$$

where $l_0 = \frac{g}{b} \geq \frac{2g\delta_1}{\pi(\pi - \delta_1)}$, $g = 9.81$ and δ_1 is a small positive constant.

3.4.5 The Upper Bound of $\frac{\partial W}{\partial y}g(x, y + h(x))$

The boundary-layer system $g(x, y + h(x))$, is

$$g(x, h(x)) = \begin{bmatrix} y_2 \\ -\frac{y_1}{m} - \alpha y_2 \end{bmatrix}$$

where $0 < \alpha < 1$ and $m > 0$. The Lyapunov function of the boundary-layer system is

$$W(x, y) = \frac{m}{2}\left(\alpha + \frac{m+1}{\alpha m^2}\right)y_1^2 + my_1y_2 + \frac{m+1}{2\alpha}y_2^2.$$

The partial derivative of $W(y)$ is

$$\frac{\partial W}{\partial y} = \left[\; m\left(\alpha + \tfrac{m+1}{\alpha m^2}\right) y_1 + m y_2 \quad m y_1 + \tfrac{m+1}{\alpha} y_2 \; \right].$$

We wish to find the upper bound of $\frac{\partial W}{\partial y} g(x, y + h(x))$, that is

$$\frac{\partial W}{\partial y} g(x, y + h(x)) = -y_1^2 - y_2^2.$$

Thus the upper bound of $\frac{\partial W}{\partial y} g(x, y + h(x))$ for $|y_1| > 0, \; |y_2| > 0$ is

$$\frac{\partial W}{\partial y} g(x, y + h(x)) \leq -\frac{1}{2} \left(|y_1| + |y_2|\right)^2$$

where $m > 0$ and $0 < \alpha < 1$.

3.4.6 The Upper and Lower Bounds of $W(x, y)$

The Lyapunov function of the boundary-layer system is

$$W(x, y) = \frac{m}{2} \left(\alpha + \frac{m+1}{\alpha m^2}\right) y_1^2 + m y_1 y_2 + \frac{m+1}{2\alpha} y_2^2$$

where $m > 0$ and $0 < \alpha < 1$. We will start to estimate the upper bound of $W(x, y)$, that is $W(x, y) \leq \zeta_2(\| \; y \; \|)$, where ζ_2 is a K function, see footnote in Appendix B. It is enough to consider the upper bound of $W(x, y)$ for the case $y_1 > 0, \; y_2 > 0$. Thus

$$\begin{aligned} &\frac{m}{2} \left(\alpha + \frac{m+1}{\alpha m^2}\right) |y_1|^2 + m|y_1||y_2| + \frac{m+1}{2\alpha} |y_2|^2 \\ &\leq \max\left(\frac{m}{2} \left(\alpha + \frac{m+1}{\alpha m^2}\right), m, \frac{m+1}{2\alpha}\right) \left(|y_1| + |y_2|\right)^2. \end{aligned}$$

We continue by estimating the lower bound of $W(x, y)$, that is $W(x, y) \geq \zeta_1(\| \; y \; \|)$, where ζ_2 is a K function. It is enough to consider the lower bound of $W(x, y)$ for the case when $y_1 > 0, \; y_2 < 0$. Thus

$$\begin{aligned} &\frac{m}{2} \left(\alpha + \frac{m+1}{\alpha m^2}\right) |y_1|^2 - m|y_1||y_2| + \frac{m+1}{2\alpha} |y_2|^2 \\ &\geq \frac{1}{2} \min\left(\frac{m}{2} \left(\alpha + \frac{m+1}{\alpha m^2}\right) - \frac{m^2}{4}, \; \frac{m+1}{2\alpha} - 1\right) \left(|y_1| + |y_2|\right)^2. \end{aligned}$$

Thus the upper bound of $W(x, y)$ for $|y_1| > 0, \; |y_2| > 0$ is

$$W(x, y) \leq \max\left(\frac{m}{2} \left(\alpha + \frac{m+1}{\alpha m^2}\right), \; m, \; \frac{m+1}{2\alpha}\right) \left(|y_1| + |y_2|\right)^2$$

and the lower bound of $W(x,y)$ for $|y_1|>0,\ |y_2|>0$ is

$$W(x,y) \geq \frac{1}{2}\min\left(\frac{m}{2}\left(\alpha+\frac{m+1}{\alpha m^2}\right)-\frac{m^2}{4},\ \frac{m+1}{2\alpha}-1\right)(|y_1|+|y_2|)^2$$

where $0<\alpha<1$. Also, the following two conditions must be fulfilled

$$\begin{aligned} m &> 2\alpha-1, \\ \alpha+\frac{m+1}{\alpha m^2} &> \frac{m}{2}. \end{aligned}$$

We see that the two conditions are satisfied for small m. The first one is trivial and the last one will be fulfilled as the left side grows as $O(\frac{1}{m})$ and the right side as $O(m)$.

3.4.7 The Upper Bound of $\| \frac{\partial V(x)}{\partial x} \|$

We have the Lyapunov function of the reduced system

$$V(x)=\frac{1}{4}\left(\frac{\eta}{m}\right)^2 x_1^2+\frac{1}{2}\left(\frac{\eta}{m}\right)x_1x_2+\frac{1}{2}x_2^2+\frac{g}{l_0}(1-\cos x_1)$$

where $m\leq 1$ and $g,\ \eta,\ l_0>0$. The partial derivative of $V(x)$ is

$$\frac{\partial V(x)}{\partial x}=\left[\ \tfrac{1}{2}\left(\tfrac{\eta}{m}\right)^2 x_1+\tfrac{1}{2}\left(\tfrac{\eta}{m}\right)x_2+\tfrac{g}{l_0}\sin x_1 \quad \tfrac{1}{2}\left(\tfrac{\eta}{m}\right)x_1+x_2\ \right],$$

where $|x_1|<\pi$.
The square of the norm of $\frac{\partial V(x)}{\partial x}$ is

$$\| \frac{\partial V(x)}{\partial x} \|^2 = \left(\frac{1}{2}\left(\frac{\eta}{m}\right)^2 x_1+\frac{1}{2}\left(\frac{\eta}{m}\right)x_2+\frac{g}{l_0}\sin x_1\right)^2+\left(\frac{1}{2}\left(\frac{\eta}{m}\right)x_1+x_2\right)^2.$$

Set $a=\frac{\eta}{m}$ and $b=\frac{g}{l_0}$.
The upper bound of $\| \frac{\partial V(x)}{\partial x} \|^2$ for the case $|x_1|<\pi,\ |x_2|\geq 0$ is

$$\begin{aligned} &\left(-\left(\frac{a^2}{2}|x_1|+b\sin|x_1|\right)+\frac{a}{2}|x_2|\right)^2+\left(-\frac{a}{2}|x_1|+|x_2|\right)^2 \\ &\quad\leq\left(\left(\frac{a^2}{2}+b\right)|x_1|+\frac{a}{2}|x_2|\right)^2+\left(\frac{a}{2}|x_1|+|x_2|\right)^2 \\ &\quad\leq 2\max\left(\left(\frac{a^2}{2}+b\right)^2,\ \left(\frac{a}{2}\right)^2,\ 1\right)(|x_1|+|x_2|)^2. \end{aligned}$$

Thus the upper bound of $\| \frac{\partial V(x)}{\partial x} \|$ for $|x_1| < \pi$, $|x_2| \geq 0$, is

$$\| \frac{\partial V(x)}{\partial x} \| \leq 2 \max \left(\left(\frac{a^2}{2} + b \right), \left(\frac{a}{2} \right), 1 \right) (|x_1| + |x_2|)$$
$$= 2 \left(\frac{a^2}{2} + b \right) (|x_1| + |x_2|).$$

Consequently, the upper bound of $\| \frac{\partial V(x)}{\partial x} \|$ for $|x_1| < \pi$, $|x_2| > 0$, is

$$\| \frac{\partial V(x)}{\partial x} \| \leq 2 \left(\left(\frac{\eta}{m} \right)^2 + \frac{g}{l_0} \right) (|x_1| + |x_2|)$$

where η, $m > 0$ and $l_0 = \frac{g}{b} \geq \frac{2g\delta_1}{\pi(\pi - \delta_1)}$ from Subsection 3.4.4.

3.4.8 The Upper Bound of $\| f(x, y + h(x)) - f(x, h(x)) \|$

Finding the upper bound of the norm of $f(x, y + h(x)) - f(x, h(x))$, where $f(x, y + h(x)) - f(x, h(x))$ is

$$f(x, y + h(x)) - f(x, h(x)) = \begin{bmatrix} 0 \\ -\frac{g}{l_0} \frac{y_1}{(l_0 + y_1)} \sin x_1 \end{bmatrix}$$

where g, $l_0 > 0$. The square of the norm of $f(x, y + h(x)) - f(x, h(x))$, is

$$\| f(x, y + h(x)) - f(x, h(x)) \|^2 = \left(\frac{g}{l_0} \right)^2 \frac{y_1^2}{(l_0 + y_1)^2} \sin^2 x_1.$$

The upper bound of $\| f(x, y + h(x)) - f(x, h(x)) \|^2$ for the case $y_1 > 0$, $|y_2| > 0$, is

$$\left(\frac{g}{l_0} \right)^2 \frac{|y_1|^2}{(l_0 + |y_1|)^2} \sin^2 |x_1|$$
$$\leq \left(\frac{\pi g}{l_0} \right)^2 \frac{|y_1|^2}{l_0^2}$$
$$\leq \left(\frac{\pi g}{l_0^2} \right)^2 (|y_1| + |y_2|)^2.$$

Here, $|x_1| < \pi$. The upper bound of $\| f(x, y + h(x)) - f(x, h(x)) \|^2$ for the case when $y_1 < l_0 - \delta_2$, where δ_2 is a small positive constant, and $|y_2| > 0$, is

$$\left(\frac{g}{l_0} \right)^2 \frac{|y_1|^2}{(l_0 - |y_1|)^2} \sin^2 |x_1|$$
$$\leq \frac{1}{\delta_2^2} \left(\frac{g}{l_0} \right)^2 |y_1|^2 \pi^2$$
$$\leq \left(\frac{g}{l_0} \right)^2 \left(\frac{\pi}{\delta_2} \right)^2 (|y_1| + |y_2|)^2.$$

Here, $|x_1| < \pi$. Thus the upper bound of $\| f(x, y + h(x)) - f(x, h(x)) \|$ for $y_1 < l_0 - \delta_2$, $|y_2| > 0$ is,

$$\| f(x, y + h(x)) - f(x, h(x)) \| \leq \left(\frac{g}{l_0}\right)\left(\frac{\pi}{\delta_2}\right)(|y_1| + |y_2|).$$

where $g = 9.81$ and $l_0 \geq \frac{2g\delta_1}{\pi(\pi-\delta_1)}$.

3.4.9 The Upper Bound of ϵ

To sum up our findings we have

$\frac{\partial V}{\partial x} f(x, h(x)) \leq -\frac{\eta g \delta_1}{2ml_0\pi(\pi-\delta_1)}(|x_1| + |x_2|)^2$,

$\frac{\partial W}{\partial y} f(x, h(x)) \leq -\frac{1}{2}(|y_1| + |y_2|)^2$,

$$\frac{\partial V}{\partial x}[f(x, y + h(x)) - f(x, h(x))] \leq 2\left(\left(\frac{\eta}{m}\right)^2 + \frac{g}{l_0}\right)\left(\frac{g}{l_0}\right)\left(\frac{\pi}{\delta_2}\right)(|x_1| + |x_2|)(|y_1| + |y_2|)$$

and $\zeta_1(\|y\|) \leq W(x, y) \leq \zeta_2(\|y\|)$ where

$$\zeta_1 = \frac{1}{2}\min\left(\frac{m}{2}\left(\alpha + \frac{m+1}{\alpha m^2}\right) - \frac{m^2}{4},\ \frac{m+1}{2\alpha} - 1\right)(|y_1| + |y_2|)^2,$$

$$\zeta_2 = \max\left(\frac{m}{2}\left(\alpha + \frac{m+1}{\alpha m^2}\right),\ m,\ \frac{m+1}{2\alpha}\right)(|y_1| + |y_2|)^2$$

if the following conditions

$$\begin{array}{rcl} l_0 & \geq & \frac{2g\delta_1}{\pi(\pi-\delta_1)}, \\ m & > & 2\alpha - 1, \\ \frac{m}{2} & < & \alpha + \frac{m+1}{\alpha m^2}. \end{array}$$

where $0 < \alpha < 1$, $g = 9.81$ and δ_1, δ_2 are small positive constants.
Comparing the conditions above with those in (B.7)-(B.8) and (B.10) in Theorem B.1 we get the wanted constants to calculate ϵ^*. That is

$$\begin{array}{rcl} \alpha_1 & = & \frac{\eta g \delta_1}{2ml_0\pi(\pi-\delta_1)}, \\ \alpha_2 & = & \frac{1}{2}, \\ \beta_1 & = & \left(\left(\frac{\eta}{m}\right)^2 + \frac{g}{l_0}\right)\left(\frac{g}{l_0}\right)\left(\frac{\pi}{\delta_2}\right). \end{array}$$

From (B.12) in Theorem B.1 we get ϵ_d. Recall that the constants β_2 and γ are equal to zero. Thus

$$\epsilon_d = \frac{\frac{\eta\delta_1}{m\pi(\pi-\delta_1)}}{\frac{(1-d)}{d}\left(\left(\frac{\eta}{m}\right)^2 + \frac{g}{l_0}\right)^2\left(\frac{g}{l_0}\right)\left(\frac{\pi}{\delta_2}\right)^2}$$

where $\epsilon_d(d)$ is a strictly increasing function for all $d \in (0,1)$. Thus, the upper bound of ϵ will be

$$\epsilon < \infty.$$

Consequently, Theorem B.1 implies that the singularly perturbed system of the energy dissipative pendulum will be asymptotically stable in the origin for all spring constants k. Recall that ϵ was chosen as $\frac{1}{\sqrt{k}}$.

3.4.10 Simulation Results of the Pendulum

Finally, we will examine if our pendulum will be asymptotically stable at the origin for all $\epsilon < \infty$. This can be done by investigating the importance of the three following conditions (i), (ii) and (iii) on α, m and l_0 when simulating our system in OmSim.

$$\begin{array}{llll} (i) & m & > & 2\alpha - 1, \\ (ii) & \frac{m}{2} & < & \alpha + \frac{m+1}{\alpha m^2}, \\ (iii) & l_0 & \geq & \frac{2g\delta_1}{\pi(\pi-\delta_1)} \end{array}$$

where $g = 9.81$.
For all simulations of the pendulum all parameters will remain fixed except the one we will investigate.

Checking for condition (i): we will examine how the viscous damping α influences the asymptotical stability of the pendulum. In this case we set the parameters to such values that the conditions (ii) and (iii) are fulfilled. Thus, only the condition (i) needs to be checked. The simulations in OmSim for different values of α will result in those upper bounds of ϵ displayed in Figure 3.3. We observe that there is an upper limit for ϵ. Furthermore, the simulation results show that the condition (i) appears to have little importance for the asymptotical stability of the pendulum.

Checking for condition (ii): we will examine how the mass of the bob m influences the asymptotical stability of the pendulum. In this case we set the parameters to such values that the conditions (i) and (iii) are fulfilled. Thus, only the condition (ii) needs to be checked. The simulations in OmSim for different values of m will result in those upper bounds of ϵ displayed in Figure 3.4. We observe that there is an upper limit for ϵ. Furthermore, we see that the upper bound of ϵ is bigger for small masses compared to larger masses. Thus, we see the importance of condition (ii) for the asymptotical stability of the system, see a detailed explanation in Subsection 3.4.6.

Checking for condition (iii): we will examine how the length of the rod, l_0, influences on the asymptotical stability of the pendulum. In this case we set the parameters to values such that the conditions (i) and (ii) are fulfilled. Thus, only the condition (iii) needs to be checked. The simulations in OmSim

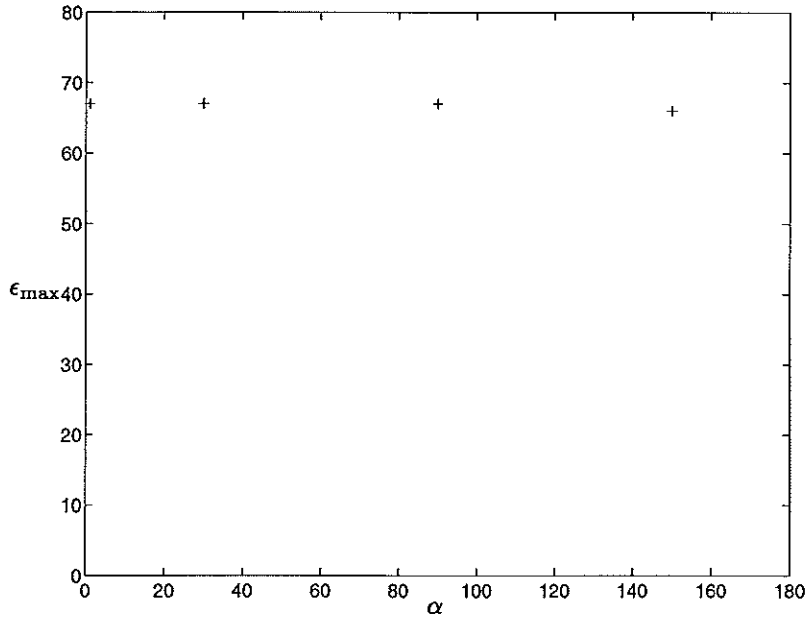

Figure 3.3: The upper bound of ϵ for different values on α for which the pendulum is asymptotically stable. The simulations have been done for $m = 1$, $\eta = 1$, $l_0 = 100$ and $\delta_1 = \delta_2 = 0.001$. The pendulum started at rest at a starting position $\theta = 60^o$.

for different l_0 will result in those upper bounds of ϵ displayed in Figure 3.5. We observe that there is an upper limit for ϵ. The condition $l_0 \geq \frac{2g\delta_1}{\pi(\pi-\delta_1)}$ appears to have little importance, because the lower bound of l_0 will always be almost zero as δ_1 is an arbitrarly small positive parameter. Consequently, condition (iii) tells us that the length of the rod can never be zero.
A possible explanation of the instability of the pendulum in real life when l_0 is large may be the following: when l_0 increases it implies a larger torque through the suspension point of the pendulum, because the lever arm is l_0+u_0+u. Thus, the tangential motion of the bob will be provided with more energy. Therefore, if ϵ is too large the total system may generate more energy than will dissipate from the system, leading to instability.

When we examined how α, m and l_0 influenced the asymptotical stability of the pendulum, each case was simulated in OmSim for two numerical methods, where each method was checked for different relative errors. The purpose was to check the numerical sensitivity when calculating the upper bound of ϵ. We used the following integration methods:

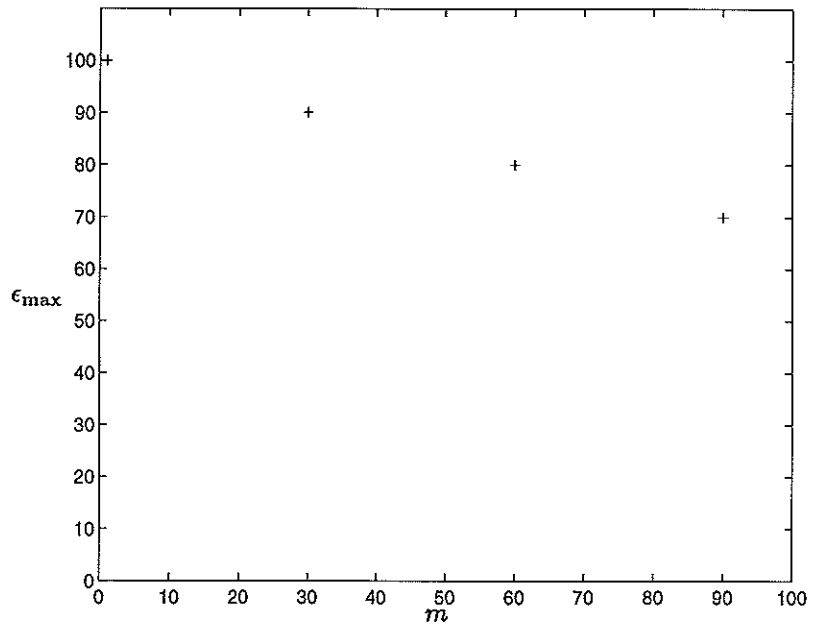

Figure 3.4: The upper bound of ϵ for different values on m for which the pendulum is asymptotically stable. The simulations have been done for $\alpha = 0.5$, $\eta = 1$, $l_0 = 100$ and $\delta_1 = \delta_2 = 0.001$. The pendulum started at rest at a starting position $\theta = 60^o$.

Dasrt Multistep, BDF methods for implicit differential-algebraic equations and stiff problems.

Radan5 Implicit Runge-Kutta method for differential-algebraic equations and stiff problems.

Independently of the choice of numerical methods or their relative errors, the upper bound of ϵ, for which the pendulum would be asymptotically stable in the origin, remained the same in each case. Yet, the theorem was applied to our system in an analytically correct way.
Hence, simulations show that there appears to be an upper limit for ϵ which probably constitutes also a limit for practical applications. Of course, this evidence does not disprove the Theorem B.1 for several reasons. Firstly, numerical stability problems can not be excluded. Secondly, simulations are made over a finite time interval.

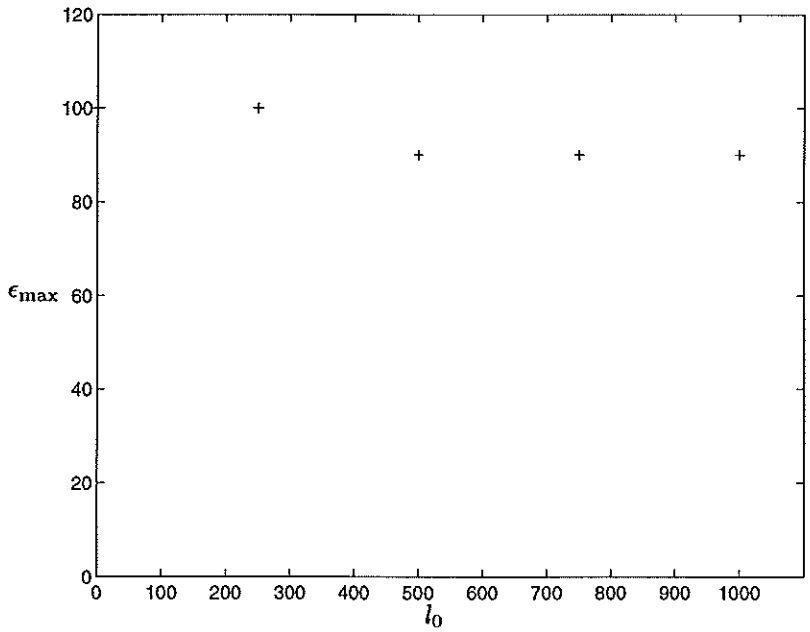

Figure 3.5: The upper bound of ϵ for different values on l_0 for which the pendulum is asymptotically stable. The simulations have been done for $\alpha = 0.5$, $\eta = 1$, $m = 5$ and $\delta_1 = \delta_2 = 0.001$. The pendulum started at rest at a starting position $\theta = 60^o$.

Chapter 4

The Possibility of Generalizing Theorem B.1

In this chapter we will try to answer the question of generalizing Theorem B.1, in the sense of neglecting some of its conditions. Consequently, the upper bound of ϵ will be raised, implying a broadening of the interval of possible ϵ, which we hope will generate an asymptotically stable behaviour of the singularly perturbed system. By examining a set of dynamical systems which are examples and exercises in Chapter 8 of [4]. We will try to answer this question. For each system Theorem B.1 will generate a valid upper bound of ϵ, that is, their singularly perturbed system is asymptotically stable in the origin. However, there is no reason to check the pendulum in Chapter 3, as the theorem did not generate a valid upper bound of ϵ.
We start by calculating the new upper bounds of ϵ by neglecting either of the interconnection conditions in the theorem. Finally, each dynamical system is examined in OmSim for these new ϵ^*. From the simulation results of the different system we will try to draw some conclusions as to the possibility of generalizing Theorem B.1.

We will know calculate the upper bounds of ϵ when neglecting either β_1 or β_2 and γ.

A Neglect β_1, then ϵ_d in (B.12) is

$$\epsilon_d(d) = \frac{\alpha_1\alpha_2}{\alpha_1\gamma + \frac{d\beta_2^2}{4(1-d)}}.$$

The function $\epsilon_d(d)$ does not have a maximum value for $d \in (0,1)$, instead it is strictly decreasing. Thus

$$\epsilon < \frac{\alpha_2}{\gamma}.$$

B Neglect β_2, γ then ϵ_d is

$$\epsilon_d(d) = \frac{\alpha_1\alpha_2}{\beta_1^2}\frac{4d}{(1-d)}.$$

The function $\epsilon_d(d)$ is a strictly increasing for $d \in (0,1)$. Thus

$$\epsilon < \infty.$$

In the following sections we will verify four different dynamical systems to see if it is possible to neglect any of the two previous conditions and still have an asymptotically stable behaviour for each of the singularly perturbed system.

4.1 Example 1

The second-order system

$$\begin{aligned} \dot{x} &= x - x^3 + z, \\ \epsilon\dot{z} &= -x - z \end{aligned}$$

has a unique equilibrium point at the origin. The equation

$$0 = -x - z$$

has a unique root $z = h(x) = -x$. We apply the change of variables $y = z + x$, to obtain

$$\begin{aligned} \dot{x} &= -x^3 + y, \\ \epsilon\dot{z} &= -y + \epsilon(-x^3 + y). \end{aligned}$$

Let $V(x) = \frac{1}{4}x^4$ and $W(y) = \frac{1}{2}y^2$. Then,

$$\frac{\partial V}{\partial x} f(x, h(x)) \leq -|x|^6 \implies \alpha_1 = 1,\ \psi_1 = |x|^3,$$

$$\frac{\partial W}{\partial y} g(x, y + h(x)) \leq -|y|^2 \implies \alpha_2 = 1,\ \psi_2 = |y|,$$

$$\frac{\partial V}{\partial x}[f(x, y + h(x)) - f(x, h(x))] \leq |x|^3|y| \implies \beta_1 = 1,$$

$$\left[\frac{\partial W}{\partial x} - \frac{\partial W}{\partial y}\frac{\partial h}{\partial x}\right] f(x, y + h(x)) \leq |x|^3|y| + |y|^2 \implies \beta_2 = \gamma = 1.$$

Hence, the origin is asymptotically stable for $\epsilon < \epsilon^*$,where

$$\epsilon^* = 0.5.$$

Put in the values of the given parameters α_1, α_2, β_1, β_2 and γ in the already calculated upper bounds of ϵ in **A-B**. We have, **A**: $\epsilon < 1$, **B**: $\epsilon < \infty$. As a result

the singularly perturbed system is suggested to be asymptotically stable at the origin for $\epsilon < 1$, instead of $\epsilon < 0.5$.
Our simulations in OmSim confirm that the singularly perturbed system is asymptotically stable in the origin for all $\epsilon < 1$. For $\epsilon \geq 1$ the origin becomes instable, because the x_1 and z variables will oscillate around zero. Compare Figure 4.1 and Figure 4.2 on the following pages.

Conclusion Consequently, the interconnection condition of the reduced system may be neglected, but not the condition of the boundary-layer system.
As a result, Theorem B.1 constitutes a restriction in this example.

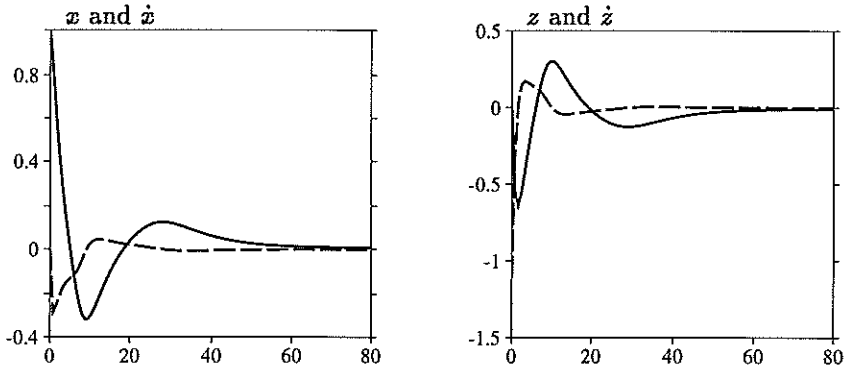

Figure 4.1: Simulation of Example 1 for $\epsilon = 0.9$, $x(0) = 1$, $\dot{x}(0) = 0$, $z(0) = 0$, $\dot{z}(0) = 0$. The solid lines show x and z while the dashed lines show their respective derivatives.

4.2 Example 2

The system

$$\begin{aligned} \dot{x} &= -x + z, \\ \epsilon\dot{z} &= \tan^{-1}(1 - x - z) \end{aligned}$$

has an unique equilibrium point at $(\frac{1}{2}, \frac{1}{2})$. The change of variables $\tilde{x} = x - \frac{1}{2}$; $\tilde{z} = z - \frac{1}{2}$ shifts the equilibrium to the origin. To simplify the notation, let us drop the tilde and write the state equation as

$$\begin{aligned} \dot{x} &= -x + z, \\ \epsilon\dot{z} &= -\tan^{-1}(x + z) \end{aligned}$$

The equation

$$0 = -\tan^{-1}(x + z)$$

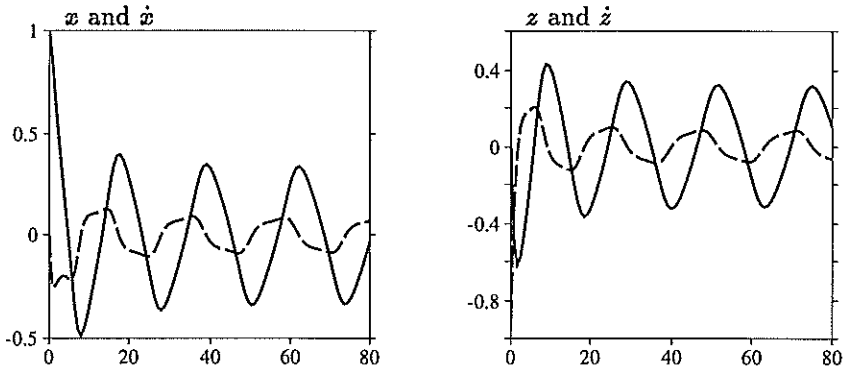

Figure 4.2: Simulation of Example 1 for $\epsilon = 1.1$, $x(0) = 1$, $\dot{x}(0) = 0$, $z(0) = 0$, $\dot{z}(0) = 0$. The solid lines show x and z while the dashed lines show their respective derivatives.

has a unique root $z = h(x) = -x$. We apply the change of variables $y = z + x$, to obtain

$$\begin{aligned} \dot{x} &= -2x + y, \\ \epsilon\dot{z} &= -\tan^{-1} y + \epsilon(-2x + y). \end{aligned}$$

Let $V(x) = \frac{1}{2}x^2$ and $W(y) = \frac{1}{2}y^2$. Then,

$$\frac{\partial V}{\partial x} f(x, h(x)) \leq -2|x|^2 \implies \alpha_1 = 2,\ \psi_1 = |x|,$$

$$\frac{\partial W}{\partial y} g(x, y + h(x)) \leq -\frac{\tan^{-1}\rho}{\rho}|y|^2,\ \forall\ |y| < \rho \implies \alpha_2 = \frac{\tan^{-1}\rho}{\rho},\ \psi_2 = |y|,$$

$$\frac{\partial V}{\partial x}[f(x, y + h(x)) - f(x, h(x))] \leq |x||y| \implies \beta_1 = 1,$$

$$\left[\frac{\partial W}{\partial x} - \frac{\partial W}{\partial y}\frac{\partial h}{\partial x}\right] f(x, y + h(x)) \leq 2|x||y| + |y|^2 \implies \beta_2 = 2,\ \gamma = 1.$$

Hence, the origin is asymptotically stable for $\epsilon < \epsilon^*$,where

$$\epsilon^* = \frac{\tan^{-1}\rho}{2\rho}.$$

The values of the parameters α_1, α_2, β_1, β_2 and γ are put in the already calculated upper bounds of ϵ in **A-B**. We have, **A**: $\epsilon < \frac{\tan^{-1}\rho}{\rho}$, **B**: $\epsilon < \infty$. As a result, the singularly perturbed system is suggested to be asymptotically stable in the origin for $\epsilon < \frac{\tan^{-1}\rho}{\rho}$, instead of $\epsilon < \frac{\tan^{-1}\rho}{2\rho}$.
Instead, our simulations in OmSim confirm that the singularly perturbed system is asymptotically stable at the origin for all ϵ, not just for $\epsilon < \frac{\tan^{-1}\rho}{\rho}$.

However, when the initial values $x(0)$ and\or $z(0)$ are large and $\epsilon > \frac{\tan^{-1}\rho}{\rho}$ the speed of convergence is slower than for $\epsilon < \frac{\tan^{-1}\rho}{\rho}$. Compare Figure 4.3, Figure 4.4 and Figure 4.5 on the following pages. Furthermore, the condition $|z + x| < \rho$ is unimportant as the system is asymptotically stable even for $|z + x| \geq \rho$.

Conclusion Consequently, the interconnection conditions may be neglected and Theorem B constitutes even in this example a restriction.

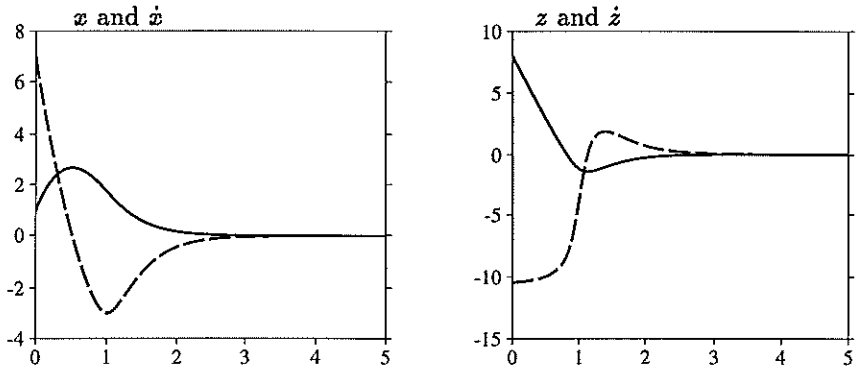

Figure 4.3: Simulation of Example 2 where the conditions $\epsilon < \frac{\tan^{-1}\rho}{\rho}$ and $|z + x| < \rho$ are valid for $\rho = 1$, $\epsilon = 0.14$, $x(0) = 1$, $\dot{x}(0) = 0$, $z(0) = 8$, $\dot{z}(0) = 0$. The solid lines show x and z while the dashed lines show their respective derivatives.

4.3 Example 3

Consider the singularly perturbed system

$$\begin{aligned} \dot{x}_1 &= x_2, \\ \dot{x}_2 &= -x_2 + z, \\ \epsilon\dot{z} &= \tan^{-1}(1 - x_1 - z) \end{aligned}$$

The system has an unique equilibrium point at $x_1 = 1$, $x_2 = z = 0$. Applying a change of variables to shift the equilibrium to the origin, we can rewrite the state equation as

$$\begin{aligned} \dot{x}_1 &= x_2, \\ \dot{x}_2 &= -x_2 + z, \\ \epsilon\dot{z} &= -\tan^{-1}(z + x_1) \end{aligned}$$

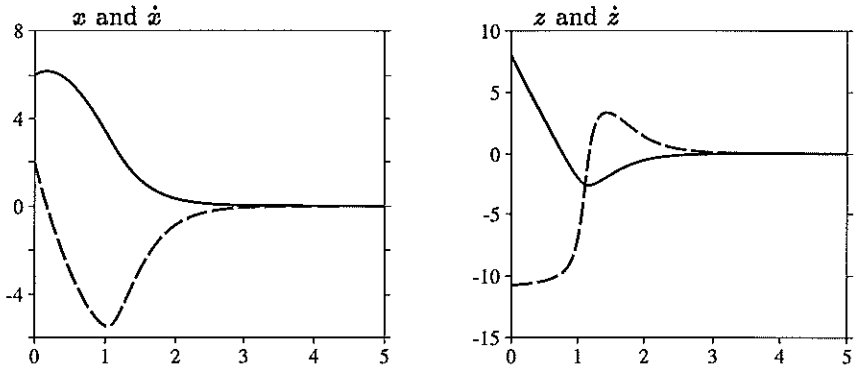

Figure 4.4: Simulation of Example 2 where the condition $|z+x| < \rho$ is not valid for $\rho = 1$, $\epsilon = 0.14$, $x(0) = 6$, $\dot{x}(0) = 0$, $z(0) = 8$, $\dot{z}(0) = 0$. The solid lines show x and z while the dashed lines show their respective derivatives.

Setting $\epsilon = 0$ yields the equation $0 = -\tan^{-1}(z + x_1)$, which has a unique root $z = h(x) = -x_1$. We apply the change of variables $y = z + x_1$, to obtain

$$\begin{aligned} \dot{x}_1 &= x_2, \\ \dot{x}_2 &= -x_1 - x_2 + y, \\ \epsilon\dot{y} &= -\tan^{-1} y + \epsilon x_2. \end{aligned}$$

The reduced model is

$$\begin{aligned} \dot{x}_1 &= x_2, \\ \dot{x}_2 &= -x_1 - x_2, \end{aligned}$$

which is the same as

$$\dot{x} = Ax.$$

The matrix A is Hurwitz. Let P be the solution of the Lyapunov equation $PA + A^T P = -I$. It is given by

$$P = \begin{bmatrix} 1.5 & 0.5 \\ 0.5 & 1 \end{bmatrix}.$$

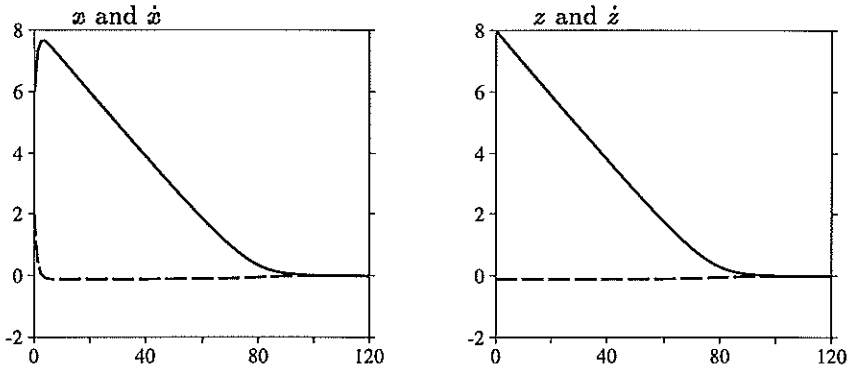

Figure 4.5: Simulation of Example 2 where the conditions $\epsilon < \frac{\tan^{-1}\rho}{\rho}$ is not valid for $\epsilon = 14$, $x(0) = 6$, $\dot{x}(0) = 0$, $z(0) = 8$, $\dot{z}(0) = 0$. The solid lines show x and z while the dashed lines show their respective derivatives.

Let $V(x) = x^T P x$ and $W(y) = \frac{1}{2}y^2$. Then,

$$\frac{\partial V}{\partial x} f(x, h(x)) = -\|x\|_2^2 \implies \alpha_1 = 1,\ \psi_1 = \|x\|_2,$$

$$\frac{\partial W}{\partial y} g(x, y + h(x)) \leq -\frac{\tan^{-1}\rho}{\rho}|y|^2,\ \forall\ |y| \leq \rho \implies \alpha_2 = \frac{\tan^{-1}\rho}{\rho},\ \psi_2 = |y|,$$

$$\frac{\partial V}{\partial x}[f(x, y + h(x)) - f(x, h(x))] \leq \sqrt{5}|x||y| \implies \beta_1 = \sqrt{5},$$

$$\left[\frac{\partial W}{\partial x} - \frac{\partial W}{\partial y}\frac{\partial h}{\partial x}\right] f(x, y + h(x)) \leq \|x\|_2|y| \implies \beta_2 = 1,\ \gamma = 0.$$

Hence, the origin is asymptotically stable for $\epsilon < \epsilon^*$,where

$$\epsilon^* = \frac{\tan^{-1}\rho}{\sqrt{5}\rho}.$$

Put in the values of the given parameters α_1, α_2, β_1, β_2 and γ in the already calculated upper bounds of ϵ in **A-B**. We have, **A**: $\epsilon < \infty$, **B**: $\epsilon < \infty$. Consequently, omitting any of the interconnection conditions will just produce the upper bound $\epsilon < \infty$.
From our simulations in OmSim the singularly perturbed system is asymptotically stable in the origin for $\epsilon < \frac{\tan^{-1}\rho}{\sqrt{5}\rho}$, $|z + x_1| < \rho$. When either of the conditions $\epsilon < \frac{\tan^{-1}\rho}{\sqrt{5}\rho}$ or $|z + x_1| < \rho$ is broken, the time of convergence to the equilibrium point will increase. If $\epsilon >> \frac{\tan^{-1}\rho}{\sqrt{5}\rho}$ is too large, the system will

blow up. To see the effects the conditions $\epsilon < \frac{\tan^{-1}\rho}{\sqrt{5}\rho}$ and $|z + x_1| < \rho$, compare Figure 4.6, Figure 4.7 and Figure 4.8 on the following pages. In Figure 4.6 the conditions $\epsilon < \frac{\tan^{-1}\rho}{\sqrt{5}\rho}$ and $|z + x_1| < \rho$ are valid, while in Figure 4.7 the condition $\epsilon < \frac{\tan^{-1}\rho}{\sqrt{5}\rho}$ is valid. Finally, in Figure 4.8 the condition $\epsilon < \frac{\tan^{-1}\rho}{\sqrt{5}\rho}$ is not valid.

Conclusion This example shows that neglecting any of the interconnection conditions will not provide a upper bound of ϵ for which the origin of the singularly perturbed system is asymptotically stable. But we can draw the conclusion that the theorem still constitutes a restriction for the upper bound of ϵ as asymptotic stability of the origin is given for $\epsilon > \epsilon^*$.

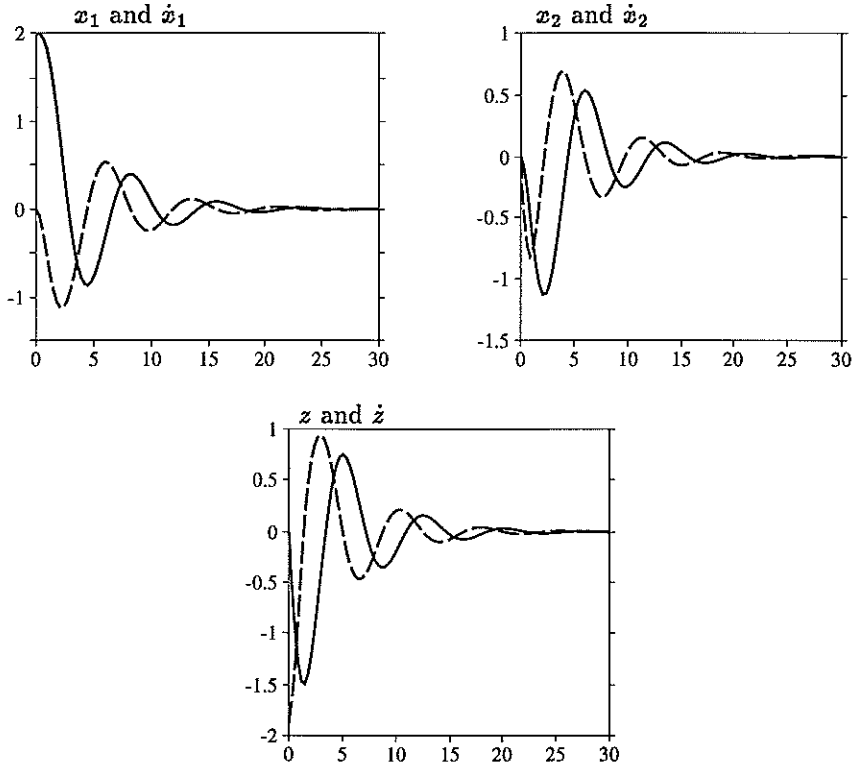

Figure 4.6: Simulation of Example 3 for $\rho = 5$, $\epsilon = 0.59$, $x_1(0) = 2$, $\dot{x}_1(0) = 0$, $x_2(0) = 0$, $\dot{x}_2(0) = 0$, $z(0) = 0$, $\dot{z}(0) = 0$. The solid lines show x and z while the dashed lines show their respective derivatives.

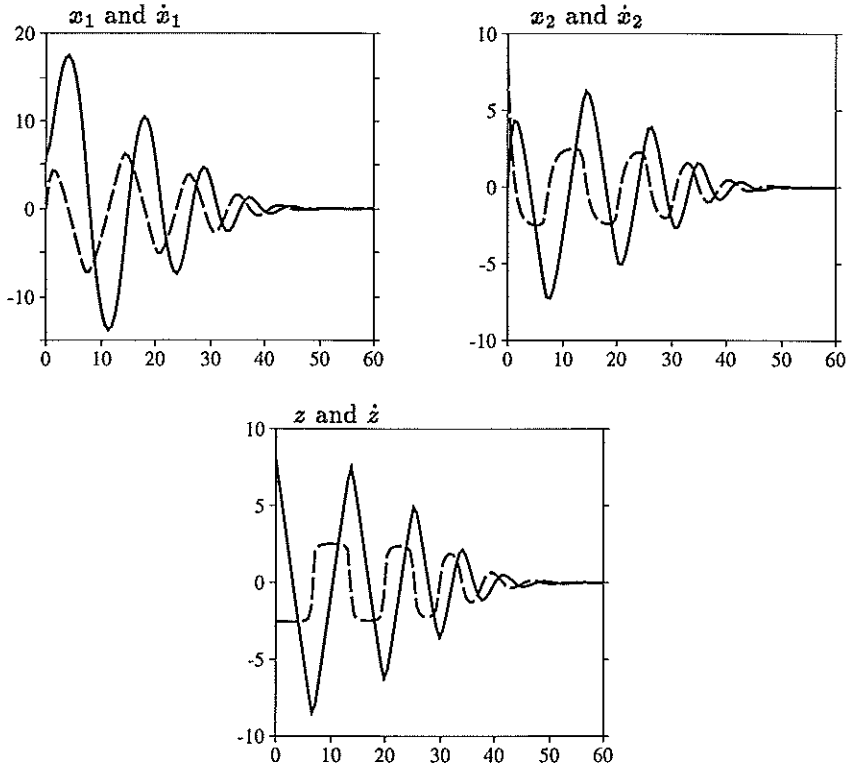

Figure 4.7: Simulation of Example 3 for $\rho = 5$, $\epsilon = 0.59$, $x_1(0) = 6$, $\dot{x}_1(0) = 0$, $x_2(0) = 0$, $\dot{x}_2(0) = 0$, $z(0) = 8$, $\dot{z}(0) = 0$. The solid lines show x and z while the dashed lines show their respective derivatives.

4.4 Example 4

The second-order system

$$\begin{aligned} \dot{x} &= -2x + x^2 + z, \\ \epsilon\dot{z} &= x - x^2 - z \end{aligned}$$

has a unique equilibrium point at the origin. The equation

$$0 = x - x^2 - z$$

has a unique root $z = h(x) = x - x^2$. We apply the change of variables $y = z - x + x^2$, to obtain

$$\begin{aligned} \dot{x} &= -x + y, \\ \epsilon\dot{z} &= -y + \epsilon(1 - 2x)(-x + y). \end{aligned}$$

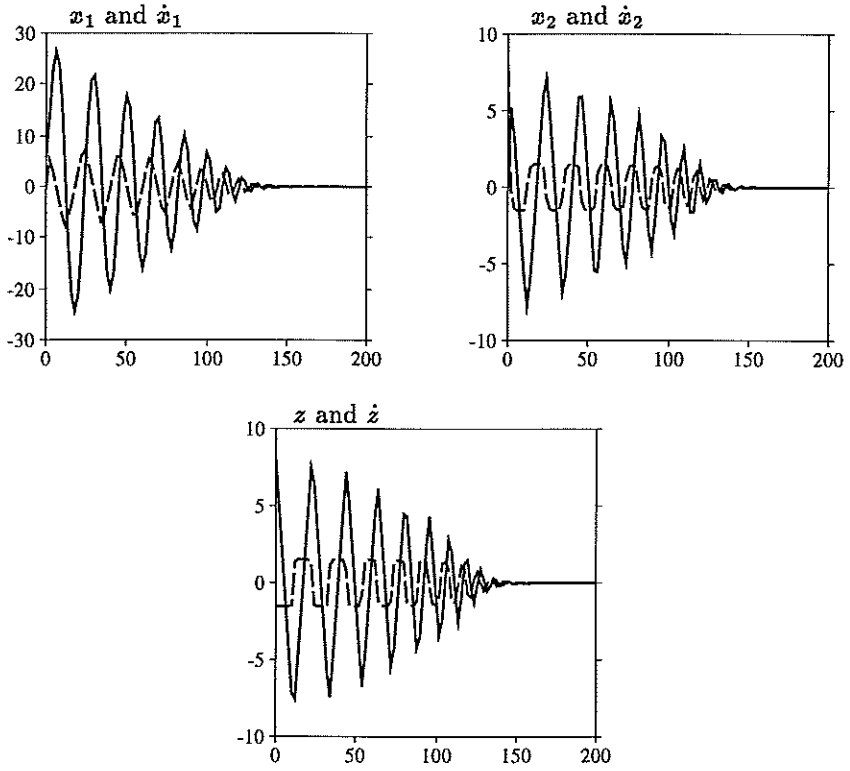

Figure 4.8: Simulation of Example 3 for $\rho = 5$, $\epsilon = 1$, $x_1(0) = 6$, $\dot{x}_1(0) = 0$, $x_2(0) = 0$, $\dot{x}_2(0) = 0$, $z(0) = 8$, $\dot{z}(0) = 0$. The solid lines show x and z while the dashed lines show their respective derivatives.

Let $V(x) = \frac{1}{2}x^2$ and $W(y) = \frac{1}{2}y^2$. Then,

$$\frac{\partial V}{\partial x} f(x, h(x)) \leq -|x|^2 \implies \alpha_1 = 1,\ \psi_1 = |x|,$$

$$\frac{\partial W}{\partial y} g(x, y + h(x)) \leq -|y|^2 \implies \alpha_2 = 1,\ \psi_2 = |y|,$$

$$\frac{\partial V}{\partial x}[f(x, y + h(x)) - f(x, h(x))] \leq |x||y| \implies \beta_1 = 1,$$

$$\left[\frac{\partial W}{\partial x} - \frac{\partial W}{\partial y}\frac{\partial h}{\partial x}\right] f(x, y + h(x)) \leq (1 + 2a)(|x||y| + |y|^2),\ \forall\ |x| \leq a \implies \beta_2 = \gamma = (1 + 2a).$$

Hence, the origin is asymptotically stable for $\epsilon < \epsilon^*$, where

$$\epsilon^* = \frac{1}{2(1+2a)}.$$

The values of the parameters α_1, α_2, β_1, β_2 and γ are put in the already calculated upper bounds of ϵ in **A-B**. We have, **A**: $\epsilon < \frac{1}{(1+2a)}$, **B**: $\epsilon < \infty$. As a result the singularly perturbed system is suggested to be asymptotically stable at the origin for $\epsilon < \frac{1}{(1+2a)}$, instead of $\epsilon < \frac{1}{2(1+2a)}$.
Our simulations in OmSim confirm that the singularly perturbed system is asymptotically stable at the origin for all $\epsilon < \frac{1}{(1+2a)}$, if the condition $|x| \leq a$ is fulfilled, see Figure 4.9.
However, when the condition $|x| \leq a$ is broken, the derivatives of $\dot{x}$ and $\dot{z}$ will be excessively large. Consequently, the system will explode. Furthermore, if the condition $\epsilon < \frac{1}{(1+2a)}$ is broken, the upper bound of $|x| \leq a$ will be lowered. Thus, in this case the previous phenomena will appear quicker.

Conclusion This example shows that the interconnection condition of the reduced system may be neglected, but not for the boundary-layer system. As it is the boundary-layer system which gives us the important restriction $|x| \leq a$.

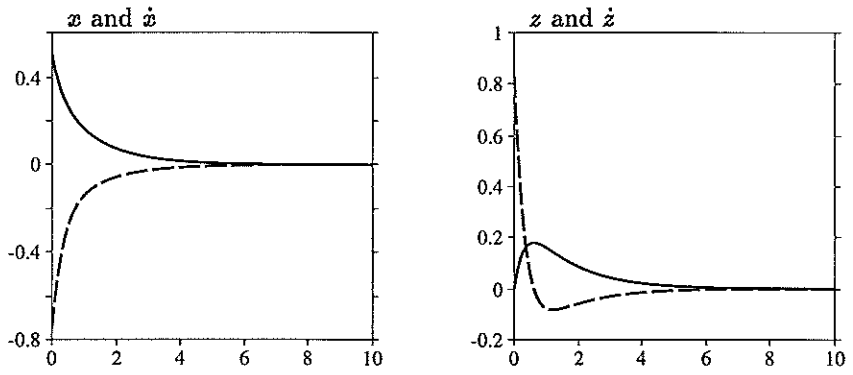

Figure 4.9: Simulation of Example 4 for $\epsilon = 0.3$, $x(0) = 0.5$, $\dot{x}(0) = 0$, $z(0) = 0$, $\dot{z}(0) = 0$. The solid lines show x and z while the dashed lines show their respective derivatives.

4.5 Conclusions of the Simulation Results

We sum up our discoveries from the four previous examples on the possibility of generalizing Theorem B.1.

Undoubtedly, the theorem constitutes a restriction on the upper bound of ϵ. Furthermore, neither of the interconnection conditions can be neglected in all examples besides in Example 2. Yet, it is difficult to come up with a general theory on the possibility of neglecting either or both interconnection conditions which will be valid for all dynamical systems.

However, from the results of our simulations on the examples, we can observe a certain pattern in the way the interconnection condition of the reduced system may be neglected. When neither of the parameters β_2 and γ are not equal to zero, this condition can be neglected. As a result, the upper bound of ϵ will be raised implying a greater interval of ϵ generating a singularly perturbed system which is asymptotically stable at the origin.

On the other hand, the interconnection condition of the boundary-layer system, is more important for Theorem B.1 compared to the interconnection condition of the reduced system. In Example 4 we saw that omitting this condition would lead to instability. The importance of this condition seems natural as it is a condition on the fast dynamics of the system, which we wish to neglect when analyzing the full-order dynamical system.

Chapter 5

Conclusions

The aim of this master thesis was to verify if Theorem B.1 could be applied to an arbitrary problem. We have chosen to examine the swinging pendulum. Furthermore, we asked if it would be possible to generalize the theorem by omitting either or both of the conditions (B.10) respectively (B.11).

Results from Chapter 2: here it was proved how essential it is to have an asymptotically stable origin for the slow model and the fast model respectively, if we want to use Theorem B.1 to our singularly perturbed system. It may seem trivial from a physical point of view that the energy conservative pendulum in Chapter 2 can never become asymptotically stable. But the results in this chapter are still significant, because, just from the theoretical results of the theorem we realize that no ϵ can be found for which the system is asymptotically stable in the origin. Thus, the theorem provides us with results that does not request any need to know the physical behaviour of the system. Therefore, this theorem is very useful in a general sense of view as no physical knowledge of the system is requested.

Results from Chapter 3: here we could apply Theorem B.1 to the energy dissipative pendulum. Even if the theorem was applied in an analytically correct way, we were not able to attain the upper bound on ϵ given by the theorem when simulating the system in OmSim. Still, our simulation results give not reasons enough to disprove the Theorem B.1. Firstly, the numerical stability of the integration methods which were available in OmSim can not be excluded. Secondly, simulations are made over a finite time interval. Furthermore, we checked the importance of the three conditions (i), (ii) and (iii), see Subsection 3.4.10, for the asymptotical stability at the origin of the pendulum. The results from the simulations proved that only the condition (ii) would be essential. Its importance was already mentioned in Subsection 3.4.6.

Results from Chapter 4: here only general conclusions could be drawn from the possibility of generalizing Theorem B.1. Yet, we made one essential conclusion that the upper bound of ϵ given by the theorem for each system we

examined constituted a restriction. Because, from the simulations in OmSim, it was shown that the asymptotic stability in the origin of the singularly perturbed system will remain for even larger ϵ, than those given by the theorem. Moreover, we could observe from our simulation results that the condition (B.10) of the slow system, could be neglected more often than the condition (B.11) of the fast system. This observation seems natural, because if the dynamics associated with the parasitic elements, that is the fast dynamics, were unstable we should not have neglected them in the first place. Because, if we neglected the fast dynamics and tried to build up a control loop to stabilize the slow model, we would only fool ourselves because the full-order model would still remain unstable.

Appendix A

Stability Theorems

Theorem A.1 *Let $x = 0$ be an equilibrium point for*

$$\dot{x} = f(x)$$

where $f : D \longrightarrow R^n$ is a locally Lipschitz map from a domain $D \subset R^n$. Let $V : D \longrightarrow R$ be a continuously differentiable function on a neighborhood D of $x = 0$, such that

$$V(0) = 0 \text{ and } V(x) > 0 \text{ in } D - \{0\} \tag{A.1}$$

$$\dot{V}(x) \leq 0 \text{ in } D \tag{A.2}$$

Then, $x = 0$ is stable. Moreover, if

$$\dot{V}(x) < 0 \text{ in } D - \{0\} \tag{A.3}$$

then, $x = 0$ is asymptotically stable.

Proof. The proof is found in [4] see p.101.

Theorem A.2 *The equilibrium point $x = 0$ of the linear time-invariant system*

$$\dot{x} = Ax$$

is stable if and only if all eigenvalues of A satisfy $Re\ \lambda_i \leq 0$ and every eigenvalue with $Re\ \lambda_i = 0$ has an associated Jordan block of order one. The equilibrium point $x = 0$ is (globally) asymptotically stable if and only if all eigenvalues of A satisfy $Re\lambda_i < 0$.

Proof: The proof is found in [4] see p.124.

Theorem A.3 *A matrix A is stability matrix, that is, Re $\lambda_i < 0$ for all eigenvalues of A, if and only if for any given positive definite symmetric matrix Q there exists a positive symmetric matrix P that satisfies the Lyapunov equation*

$$PA + A^T P = -Q. \tag{A.4}$$

Moreover, if A is a stability matrix, then P is the unique solution of (A.4).

Proof: The proof is found in [4] see p.127-128.

Appendix B

Khalil's Stability Theorem for Singularly Perturbed Systems

This is a review of Theorem 8.2 in [4], p.460-465.
We consider the autonomous singularly perturbed system

$$\dot{x} = f(x, z), \tag{B.1}$$
$$\epsilon \dot{z} = g(x, z) \tag{B.2}$$

and assume that $x = 0$, $z = 0$ is an isolated equilibrium point and the functions f and g are locally Lipschitz in an open connected set that contains the origin. We want to analyze stability of the origin by examining the reduced and boundary-layer models. Let $z = h(x)$ be an isolated root of

$$0 = g(x, z)$$

defined for all $x \in D_1 \subset R^n$, where D_1 is an open connected set that contains $x = 0$. Suppose $h(0) = 0$. If $z = h(x)$ is the only root of $0 = g$, then it must vanish at the origin since $g(0, 0) = 0$. If their are two or more isolated roots, then one of them must vanish at $x = 0$ and that is the one we must work with. We apply the change of variables $y = z - h(x)$, because this change shifts the equilibrium of the boundary-layer model to the origin. In the new coordinates, the singularly perturbed system is

$$\dot{x} = f(x, y + h(x)) \tag{B.3}$$
$$\epsilon \dot{y} = g(x, y + h(x)) - \epsilon \frac{\partial h}{\partial x} f(x, y + h(x)) \tag{B.4}$$

Assuming that $\|h(x))\| \leq \zeta(\|x\|)\ \forall\ x \in D_1$, where ζ is a class K function[1], the map $y = z - h(x)$ is stability preserving; that is, the origin of (B.1)-(B.2) is asymptotically stable if and only if the origin of (B.3)-(B.4) is asymptotically stable. The reduced system

$$\dot{x} = f(x, h(x)) \tag{B.5}$$

has the equilibrium at $x = 0$, and the boundary-layer system

$$\frac{\partial y}{\partial \tau} = g(x, y + h(x)) \tag{B.6}$$

where $\tau = \frac{t}{\epsilon}$ and x is treated as a fixed parameter, has equilibrium at $y = 0$.

Theorem B.1 *Consider the singularly perturbed system (B.3)-(B.4). Assume there are Lyapunov functions $V(x)$ and $W(x, y)$. Let $V(x)$ be a Lyapunov function for the reduced system (B.5) such that*

$$\frac{\partial V}{\partial x} f(x, h(x)) \leq -\alpha_1 \psi_1^2(x) \tag{B.7}$$

$\forall\ x \in D_1$, where $\psi_1 : R^n \longrightarrow R$ is a positive definite function.
Let $W(x, y)$ be a Lyapunov function for the boundary-layer system (B.6) such that

$$\frac{\partial W}{\partial y} g(x, y + h(x)) \leq -\alpha_2 \psi_2^2(y) \tag{B.8}$$

$\forall\ (x, y) \in D_1 \times D_2$, where $D_2 \in R^m$ is an open connected set that contains $y = 0$, and $\psi_2 : R^m \longrightarrow R$ is a positive definite function. We assume that $W(x, y)$ satisfies

$$\zeta_1(|y|) \leq W(x, y) \leq \zeta_2(|y|),\ \forall\ (x, y) \in D_1 \times D_2 \tag{B.9}$$

for some K functions ζ_1 and ζ_2.
Let $V(x)$ and $W(x, y)$ also satisfy the following two conditions

$$\frac{\partial V}{\partial x}[f(x, y + h(x)) - f(x, h(x))] \leq \beta_1 \psi_1(x) \psi_2(y) \tag{B.10}$$

and

$$\left[\frac{\partial W}{\partial x} - \frac{\partial W}{\partial y}\frac{\partial h}{\partial x}\right] f(x, y + h(x)) \leq \beta_2 \psi_1(x) \psi_2(y) + \gamma \psi_2^2(y). \tag{B.11}$$

[1] A continuous function $\alpha : [0, a) \longrightarrow [0, \infty)$ is said to belong to class K if it is strictly increasing and $\alpha(0) = 0$.

Let ϵ_d and ϵ^* be defined by

$$\epsilon_d = \frac{\alpha_1\alpha_2}{\alpha_1\gamma + \frac{1}{4d(1-d)}[(1-d)\beta_1 + d\beta_2]^2} \tag{B.12}$$

$$\epsilon^* = \frac{\alpha_1\alpha_2}{\alpha_1\gamma + \beta_1\beta_2}. \tag{B.13}$$

Then the origin of (B.3)-(B.4) is asymptotically stable for all $0 < \epsilon < \epsilon^*$. Moreover, $\nu(x,y)$, which is defined by

$$\nu(x,y) = (1-d)V(x) + dW(x,y),\ 0 < d < 1 \tag{B.14}$$

is a Lyapunov function for $\epsilon \in (0, \epsilon_d)$.

The outline of the proof is to assume that, for each of the two systems (B.5)-(B.6), the origin is asymptotically stable, and we have a Lyapunov function $V(x)$ and $W(x,y)$ that satisfies the conditions of Lyapunov's theorem. In the case of the boundary-layer system, we require asymptotic stability of the origin to hold uniformly in the frozen parameter x. That is (B.6) will satisfy

$$\|y(\tau)\| \leq \beta(y(0),\tau),\ \forall x \in D_1$$

where β is a class KL function[2]. This condition will be fulfilled if the Lyapunov function $W(x,y)$ will satisfy (B.9).
Viewing the full singularly perturbed system (B.3)-(B.4) as an interconnection of the reduced and the boundary-layer system, a composite Lyapunov candidate will be formed for the full system as a linear combination of $V(x)$ and $W(x,y)$, see (B.14).
We then proceed to calculate the derivative of (B.14) along the trajectories of the full system and verify, under reasonable growth conditions on f and g, that is the conditions (B.7)-(B.9) and (B.10)-(B.11), the composite Lyapunov function will satisfy the conditions of Lyapunov's theorem for sufficiently small ϵ.
Some interesting observations can be made on the conditions (B.10)-(B.11) which are referred to as the interconnection conditions. The first of these two terms

$$\frac{\partial V}{\partial x}[f(x, y + h(x)) - f(x, h(x))]$$

represents the effect of deviation of (B.3) from the reduced system (B.5). The other term

$$\left[\frac{\partial W}{\partial x} - \frac{\partial W}{\partial y}\frac{\partial h}{\partial x}\right] f(x, y + h(x))$$

[2]A continuous function $\beta : [0,a) \times [0,\infty) \longrightarrow [0,\infty)$ is said to belong to a class KL if for each fixed s the mapping $\beta(r,s)$ belongs to class K with respect to r, and for each fixed r the mapping $\beta(r,s)$ is decreasing with respect to s and $\beta(r,s) \longrightarrow 0$ as $s \longrightarrow \infty$.

represents the deviation of (B.4) from the boundary-layer system (B.6), as well as the effect of freezing x during the boundary-layer analysis. Notice that the interconnection conditions will be satisfied if

$$\| \frac{\partial V}{\partial x} \| \leq k_1 \psi_1(x), \tag{B.15}$$

$$\| f(x, h(x)) \| \leq k_2 \psi_1(x), \tag{B.16}$$

$$\| f(x, y + h(x)) - f(x, h(x)) \| \leq k_3 \psi_2(y), \tag{B.17}$$

$$\| \frac{\partial W}{\partial y} \| \leq k_4 \psi_2(y), \tag{B.18}$$

$$\| \frac{\partial W}{\partial x} \| \leq k_5 \psi_2(y). \tag{B.19}$$

Bibliography

[1] Andersson, M.: *OmSim and Omola, Tutorial and User's Manual, Version 3.4.* Department of Automatic Control, Lund Institute of Technology, March 1995.

[2] Bueche, F. J.: *Introduction to Physics for Scientists and Engineers.* McGraw-Hill Book Co., Singapore 1986.

[3] Glad, T. and L. Ljung: *Reglerteknik, Grundläggande teori.* Studentlitteratur, Lund 1989.

[4] Khalil, H. K.: *Nonlinear Systems.* MacMillan Publishing Company, New York 1992.

[5] Priestly, H. A.: *Introduction to Complex Analysis.* Clarendon Press, Oxford 1992.

[6] Spanne, S.: *Föreläsningar i Matristeori.* Matematiska Institutionen, Lunds Tekniska Högskola 1994.